ISSN 007-2621

No. 4 — 1984

published quarterly

Technical Review

To Advance Techniques in Acoustical, Electrical and Mechanical Measurement

Calculation of Luminance Contrast

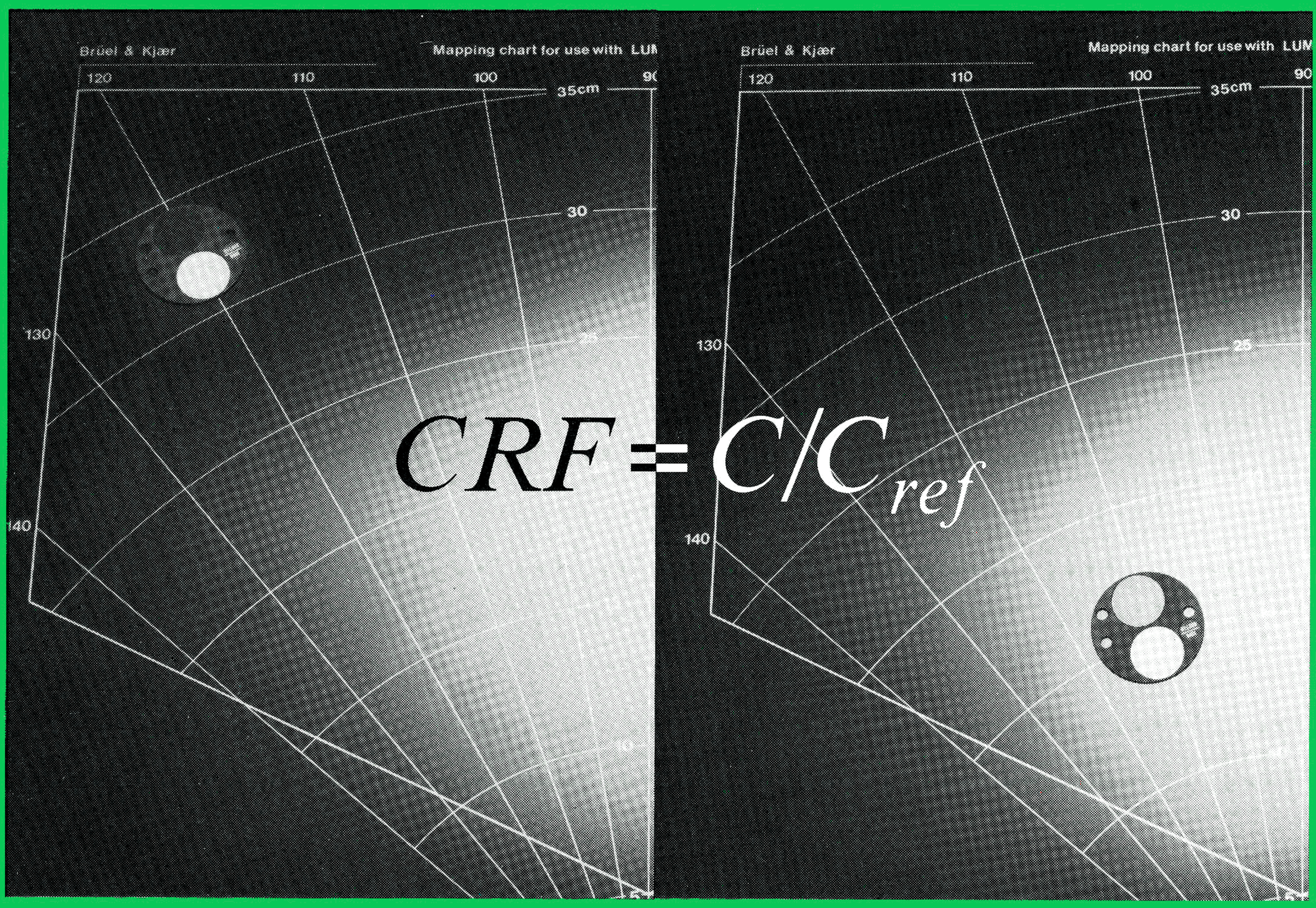

Weighting Functions for Impact Testing

Brüel & Kjær

PREVIOUSLY ISSUED NUMBERS OF BRÜEL & KJÆR TECHNICAL REVIEW

3-1984 The Hilbert Transform
Microphone System for Extremely Low Sound Levels
Averaging Times of Level Recorder 2317
2-1984 Dual Channel FFT Analysis (Part II)
1-1984 Dual Channel FFT Analysis (Part I)
4-1983 Sound Level Meters – The Atlantic Divide
Design principles for Integrating Sound Level Meters
3-1983 Fourier Analysis of Surface Roughness
2-1983 System Analysis and Time Delay Spectrometry (Part II)
1-1983 System Analysis and Time Delay Spectrometry (Part I)
4-1982 Sound Intensity (Part II Instrumentation and Applications)
Flutter Compensation of Tape Recorded Signals for Narrow Band Analysis
3-1982 Sound Intensity (Part I Theory).
2-1982 Thermal Comfort.
1-1982 Human Body Vibration Exposure and its Measurement.
4-1981 Low Frequency Calibration of Acoustical Measurement Systems.
Calibration and Standards. Vibration and Shock Measurements.
3-1981 Cepstrum Analysis.
2-1981 Acoustic Emission Source Location in Theory and in Practice.
1-1981 The Fundamentals of Industrial Balancing Machines and their Applications.
4-1980 Selection and Use of Microphones for Engine and Aircraft Noise Measurements.
3-1980 Power Based Measurements of Sound Insulation.
Acoustical Measurement of Auditory Tube Opening.
2-1980 Zoom-FFT.
1-1980 Luminance Contrast Measurement.
4-1979 Prepolarized Condenser Microphones for Measurement Purposes.
Impulse Analysis using a Real-Time Digital Filter Analyzer.
3-1979 The Rationale of Dynamic Balancing by Vibration Measurements.
Interfacing Level Recorder Type 2306 to a Digital Computer.
2-1979 Acoustic Emission.
1-1979 The Discrete Fourier Transform and FFT Analyzers.
4-1978 Reverberation Process at Low Frequencies.
3-1978 The Enigma of Sound Power Measurements at Low Frequencies.
2-1978 The Application of the Narrow Band Spectrum Analyzer Type 2031 to the Analysis of Transient and Cyclic Phenomena.
Measurement of Effective Bandwidth of Filters.

(Continued on cover page 3)

TECHNICAL REVIEW

No. 4 — 1984

Contents

Methods for the Calculation of Contrast
by Kai Sørensen, Ole Nielsen and Lars Agesen 3

Proper Use of Weighting Functions for Impact Testing
by Richard C. Sohaney and James M. Nieters 21

Computer Data Acquisition from B&K Digital Frequency Analyzers 2131/2134 using their Memory as a Buffer
by Richard J. Fridrich 32

News from the Factory 37

METHODS FOR THE CALCULATION OF CONTRAST
(The Facet Model)

by

Kai Sørensen, Ole Nielsen
and
Lars Agesen

ABSTRACT

An expression for the luminance factor matrix of glass-covered surfaces, such as those used for the Brüel & Kjær reflectance standard, is formulated, and the parameters of the expression are determined, so that a close reproduction of the measured data of the standards is obtained.

A compact method is based on the expression, which is well-suited for computer calculations of contrast conditions. Other practical problems of such calculations are considered also, and advice on practicable methods is given.

SOMMAIRE

Cet article présente une expression de la matrice du facteur de luminance de surfaces recouvertes d'une couche de verre, comme celles du contraste Etalon Bruel & Kjaer. Les paramètres de l'expression sont déterminés, de sorte qu'on obtient une reproduction fidèle des données mesurées de l'étalon.

Une méthode concise est basée sur cette expression, qui convient bien pour les calculs des conditions de contraste par ordinateur. Les problèmes pratiques se présentant lors de ces calculs sont également pris en compte, et des conseils sur des métodes pratiques sont donnés.

ZUSAMMENFASSUNG

Die Leuchtdichtefaktormatrix glasüberzogener Oberflächen, wie man sie beim Leuchtdichte-Kontrastnormal von Brüel & Kjær findet, wird in einer Gleichung erfaßt. Deren Parameter werden hinsichtlich der bestmöglichen Reproduzierbarkeit von mit dem Normal gemessenen Werten bestimmt.

Eine geeignete Methode zur Bestimmung des Leuchtdichtefaktors, die sich auf diese auch für Computerberechnungen geeignete Gleichung stützt, wird beschrieben. Außerdem werden in der Praxis auftretende Probleme solcher Berechnungen betrachtet und praktikable Methoden diskutiert.

1. Introduction

The concepts of contrast conditions in paperwork seem to be well-established and is now given in the Guide to Interior Lighting, CIE-Report No. 29/2.

It is highly advantageous to base quality criteria as well as measurements and calculations on standard surfaces, which are to simulate typical reflection properties of paper and of printed details.

For measuring purposes, a contrast standard, like the one manufactured by Brüel & Kjær, Fig.1, is useful, as it is stable and accurate, and as some data are already obtained by means of it. The "missing link", in this field is a procedure for calculating contrast conditions, in order to take these into account already at the stage of designing lighting installations or even luminaires.

The immediate need concerning the standard is convenient methods for obtaining the luminance factors to be used in calculations. In this paper a mathematical method for obtaining the luminance factors is presented.

Some definitions and concepts are summarized in Section 2, where a general discussion of contrast calculations is also given. The actual method is formulated and explained in Section 3. The starting point of the formulation is the construction of the surfaces and physics of specular and diffuse reflection. This leads to a general expression for the luminance factor for reflecting surfaces of this type. The parameters of the expression are then fitted so as to duplicate the measured luminance factors to the best possible accuracy. Finally, after some practical modifications the method is given in a compact form.

The method is believed to eliminate the most serious obstacle to performing contrast calculations. Other practical difficulties are pointed out in Section 4, and for these some advice is given.

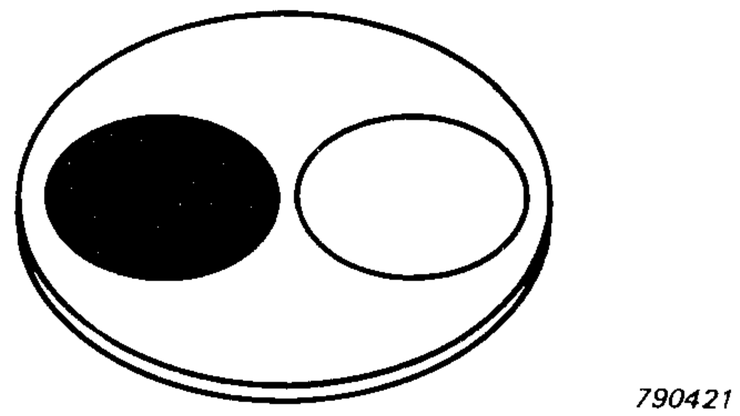

Fig. 1. Brüel & Kjær reflectance standard

The light surface simulates typical reflection properties of paper, while the dark surface simulates typical reflection properties of letters and other dark details. When used with the contrast meter, the surfaces are brought one at a time into the measuring position.

2. Definitions and general discussion of contrast calculations

When the luminance of the light paper is denoted by L_1 and the luminance of the letters or other printed dark details is denoted by L_2, the contrast is given by:

$$C = \frac{L_2 - L_1}{L_1}$$

Contrast conditions are often specified by the contrast rendering factor, *CRF*, which is the contrast in the actual situation of illumination and observation, C, divided by the reference contrast, C_{ref}.

$$CRF = C/C_{ref}$$

The reference contrast is the contrast of the visual task in a diffuse illumination. For the Brüel & Kjær reflectance standard, the value of 0,91 applies.

When further the illumination comes from a single, small light source, the luminance of a surface in a specific geometry can be found by:

$$L = \beta \times \frac{E}{\pi}$$

where β is the **luminance factor** for that geometry and E is the illuminance contribution from the source (see Fig.2).

The illuminance can be calculated by techniques which are well-known and therefore not discussed here. Further, when there is more than one small light source, the total luminance is found by summing up the contributions from each of these, as given by the above expression.

One difficulty in practice is that a light source, such as a luminaire for fluorescent tubes, is often not small in the sense that a well-defined luminance factor applies to its illumination. This difficulty is overcome by

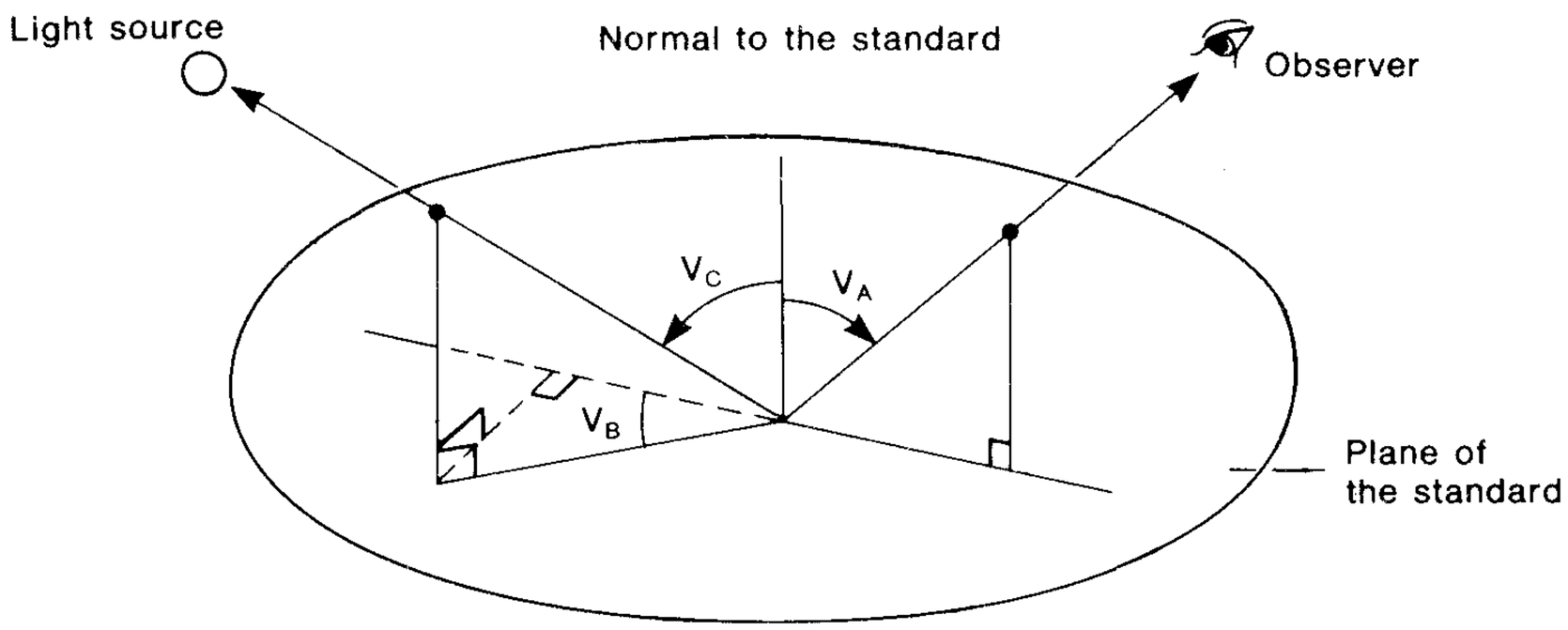

831702

Fig. 2. Angular system for specifying the geometry of illumination and observation
V_A = viewing angle
V_C = angle of incidence
V_B = azimuthal angle (angle between the planes of illumination and observation).

summing up contributions from smaller parts of the luminaire. Therefore, contrast calculations can be carried out, when the luminance factors are known for all relevant geometries for both the object (the letters) and the background (the paper). For the Brüel & Kjær reflectance standard, the luminance factors are given in the form of Tables in the angles V_A, V_B and V_C, see Tables 1 & 2 and Fig.2.

For the dark surface it can be seen that the luminance factor is small except for angles corresponding to a geometry of specular reflection ($V_C \approx V_A$ and $V_B \approx 0°$). This is interpreted in the manner that the dark surface has a small diffuse reflection, but a strong and rather narrow peak of specular reflection.

Similarly it can be seen that the light surface has a much stronger diffuse reflection, which is overlapped by a weaker and broader specular peak.

It is, therefore, obvious that the contrast will be low in situations where a luminaire is in a position to illuminate the surface in a specular direction. In other situations, the contrast will be high. It might be thought that the many values of the tables must define the total set of reflection properties to a good accuracy.

V_A	V_B \ V_C	0	3	5	7	10	15	20	25	30	35	40	45	50	60	70	80
$V_A = 5°$	0	1,480	1,669	1,718	1,696	1,537	1,190	0,959	0,852	0,801	0,775	0,760	0,748	0,737	0,708	0,655	0,534
	5	1,480	1,667	1,712	1,690	1,501	1,180	0,959	0,851	0,801	0,774	0,759	0,747	0,736	0,707	0,655	0,530
	10	1,480	1,663	1,706	1,681	1,515	1,170	0,953	0,849	0,798	0,772	0,757	0,746	0,735	0,706	0,653	0,530
	20	1,480	1,649	1,656	1,651	1,485	1,148	0,944	0,843	0,789	0,771	0,756	0,744	0,734	0,706	0,653	0,530
	50	1,480	1,567	1,552	1,489	1,322	1,045	0,894	0,820	0,781	0,763	0,750	0,740	0,730	0,702	0,650	0,529
	90	1,480	1,430	1,350	1,259	1,105	0,915	0,832	0,790	0,767	0,753	0,743	0,734	0,726	0,698	0,647	0,529
	120	1,480	1,310	1,230	1,140	1,010	0,855	0,809	0,779	0,760	0,750	0,742	0,734	0,726	0,698	0,647	0,529
	180	1,480	1,300	1,210	1,120	0,995	0,850	0,789	0,771	0,758	0,749	0,742	0,734	0,726	0,698	0,647	0,529

790153

V_A	V_B \ V_C	0	5	10	15	20	23	25	27	30	35	40	45	50	60	70	80
$V_A = 25°$	0	0,804	0,859	0,977	1,234	1,663	1,881	1,954	1,921	1,757	1,347	1,050	0,909	0,839	0,764	0,700	0,573
	5	0,804	0,856	0,971	1,218	1,625	1,823	1,880	1,847	1,691	1,308	1,035	0,900	0,834	0,763	0,698	0,571
	10	0,804	0,855	0,965	1,194	1,520	1,686	1,707	1,686	1,531	1,218	1,000	0,885	0,824	0,760	0,696	0,570
	20	0,804	0,852	0,943	1,101	1,270	1,319	1,319	1,275	1,190	1,021	0,906	0,841	0,802	0,749	0,689	0,564
	50	0,804	0,828	0,851	0,864	0,855	0,843	0,835	0,825	0,811	0,792	0,776	0,763	0,752	0,722	0,670	0,549
	90	0,804	0,798	0,788	0,778	0,769	0,765	0,762	0,759	0,755	0,750	0,745	0,737	0,730	0,704	0,655	0,545
	120	0,804	0,785	0,771	0,764	0,754	0,752	0,750	0,748	0,745	0,741	0,737	0,731	0,725	0,701	0,649	0,529
	180	0,804	0,776	0,756	0,755	0,752	0,750	0,748	0,745	0,741	0,737	0,737	0,725	0,725	0,700	0,648	0,528

790154

V_A	V_B \ V_C	0	10	15	20	25	30	35	40	43	45	47	50	55	60	70	80
$V_A = 45°$	0	0,744	0,762	0,783	0,823	0,908	1,106	1,552	2,400	2,885	3,087	3,142	2,857	2,068	1,501	1,025	0,786
	5	0,744	0,762	0,783	0,821	0,901	1,081	1,470	2,117	2,432	2,580	2,546	2,355	1,784	1,358	0,983	0,760
	10	0,744	0,761	0,781	0,815	0,884	1,019	1,266	1,577	1,687	1,726	1,696	1,590	1,322	1,114	0,893	0,710
	20	0,744	0,760	0,775	0,799	0,837	0,891	0,950	0,989	0,988	0,982	0,969	0,941	0,891	0,846	0,758	0,622
	50	0,744	0,751	0,755	0,757	0,759	0,758	0,756	0,753	0,749	0,747	0,745	0,740	0,730	0,716	0,667	0,548
	90	0,744	0,741	0,739	0,736	0,735	0,733	0,729	0,727	0,724	0,722	0,720	0,717	0,705	0,695	0,645	0,532
	120	0,744	0,736	0,733	0,731	0,728	0,726	0,723	0,721	0,717	0,715	0,713	0,711	0,693	0,686	0,638	0,521
	180	0,744	0,733	0,730	0,728	0,725	0,723	0,721	0,717	0,715	0,713	0,711	0,693	0,686	0,684	0,636	0,519

790155

Table. 1. Luminance factor for the light reflectance surface

V_A	V_B \ V_C	0	3	5	7	10	15	20	25	30	35	40	45	50	60	70	80
$V_A = 5°$	0	1,150	1,767	1,924	1,822	1,265	0,485	0,191	0,090	0,052	0,034	0,026	0,021	0,019	0,016	0,016	0,014
	5	1,150	1,760	1,911	1,805	1,236	0,480	0,190	0,090	0,052	0,034	0,026	0,021	0,019	0,016	0,016	0,014
	10	1,150	1,743	1,882	1,768	1,198	0,468	0,184	0,087	0,051	0,034	0,026	0,021	0,019	0,016	0,016	0,014
	20	1,150	1,691	1,799	1,660	1,130	0,446	0,179	0,085	0,051	0,034	0,026	0,021	0,019	0,016	0,016	0,014
	50	1,150	1,395	1,353	1,144	0,733	0,290	0,127	0,068	0,041	0,028	0,023	0,019	0,017	0,016	0,015	0,014
	90	1,150	1,000	0,803	0,588	0,365	0,153	0,078	0,046	0,031	0,023	0,019	0,017	0,016	0,015	0,014	0,013
	120	1,150	0,750	0,540	0,395	0,240	0,106	0,058	0,036	0,026	0,021	0,017	0,016	0,015	0,014	0,014	0,013
	180	1,150	0,640	0,435	0,300	0,175	0,083	0,047	0,031	0,024	0,020	0,017	0,015	0,014	0,014	0,014	0,013

790150

V_A	V_B \ V_C	0	5	10	15	20	23	25	27	30	35	40	45	50	60	70	80
$V_A = 25°$	0	0,050	0,092	0,203	0,545	1,471	2,160	2,350	2,226	1,579	0,631	0,257	0,129	0,078	0,043	0,032	0,025
	5	0,050	0,092	0,202	0,527	1,369	1,975	2,105	1,975	1,394	0,572	0,242	0,124	0,076	0,042	0,032	0,025
	10	0,050	0,091	0,194	0,482	1,120	1,507	1,566	1,441	1,030	0,454	0,208	0,111	0,070	0,040	0,030	0,025
	20	0,050	0,087	0,170	0,348	0,600	0,672	0,659	0,583	0,447	0,230	0,129	0,079	0,054	0,035	0,028	0,024
	50	0,050	0,068	0,087	0,097	0,090	0,080	0,073	0,066	0,055	0,042	0,033	0,027	0,023	0,020	0,019	0,016
	90	0,050	0,046	0,040	0,033	0,027	0,024	0,022	0,021	0,019	0,017	0,016	0,015	0,014	0,014	0,014	0,013
	120	0,050	0,037	0,028	0,022	0,019	0,017	0,016	0,015	0,015	0,014	0,013	0,013	0,013	0,013	0,013	0,011
	180	0,050	0,031	0,022	0,019	0,017	0,016	0,015	0,015	0,014	0,013	0,012	0,012	0,012	0,012	0,012	0,011

790151

V_A	V_B \ V_C	0	10	15	20	25	30	35	40	43	45	47	50	55	60	70	80
$V_A = 45°$	0	0,017	0,028	0,042	0,069	0,134	0,312	0,893	2,656	4,207	4,815	4,650	3,328	1,429	0,648	0,255	0,156
	5	0,017	0,028	0,041	0,067	0,127	0,281	0,734	1,868	2,662	2,879	2,721	2,069	1,007	0,513	0,222	0,141
	10	0,017	0,028	0,040	0,064	0,114	0,227	0,473	0,874	1,050	1,067	0,985	0,816	0,495	0,307	0,162	0,111
	20	0,017	0,027	0,036	0,053	0,080	0,121	0,169	0,198	0,199	0,192	0,181	0,162	0,128	0,102	0,073	0,058
	50	0,017	0,022	0,024	0,026	0,027	0,027	0,026	0,025	0,024	0,024	0,024	0,023	0,023	0,023	0,022	0,021
	90	0,017	0,016	0,016	0,015	0,015	0,015	0,015	0,015	0,015	0,015	0,015	0,015	0,015	0,015	0,015	0,014
	120	0,017	0,015	0,014	0,013	0,013	0,013	0,013	0,013	0,013	0,013	0,013	0,013	0,013	0,013	0,013	0,012
	180	0,017	0,013	0,013	0,013	0,012	0,012	0,012	0,012	0,012	0,012	0,012	0,012	0,012	0,012	0,012	0,011

790152

Table. 2. Luminance factor for the dark reflectance surface

However, the tables are not sufficiently detailed to allow accurate interpolation of luminance factors in random geometries. Therefore, another method for obtaining the luminance factors is needed for contrast calculations.

It has been attempted to set up larger and more elaborate tables for this purpose. It was found, however, that such tables will become very bulky and that complicated interpolation methods will be required. In fact, the luminance factor, which is a rapidly varying function of three angles, is not easily tabulated in detail. Instead of more detailed tables, a method is therefore proposed which is based on the actual physics of reflection in the surfaces of the standard. This method is explained in Section 3, where an expression for the luminance factors is formulated. The expression contains a number of parameters, which are fitted so as to reproduce the data of Table 1 and 2 to the best possible accuracy.

The method is found to be both fast on the computer and sufficiently accurate. The proposal is to be understood in the sense that the Tables 1 and 2 still define the standard, but that for calculation purposes the tables are substituted by the expression. Similarly, in measurements the tables are substituted by the used reflectance standard. By this proposal, the basic difficulty in performing contrast calculations is believed to be overcome. Other difficulties relate to the amount of computing to be carried out.

Thus the contrast conditions are usually evaluated for a field in which the *CRF* varies from point to point, see Fig.3. Further, in offices there are often several locations of desks and possibly more than one orientation of these. The computing time will easily pose a problem, and the various

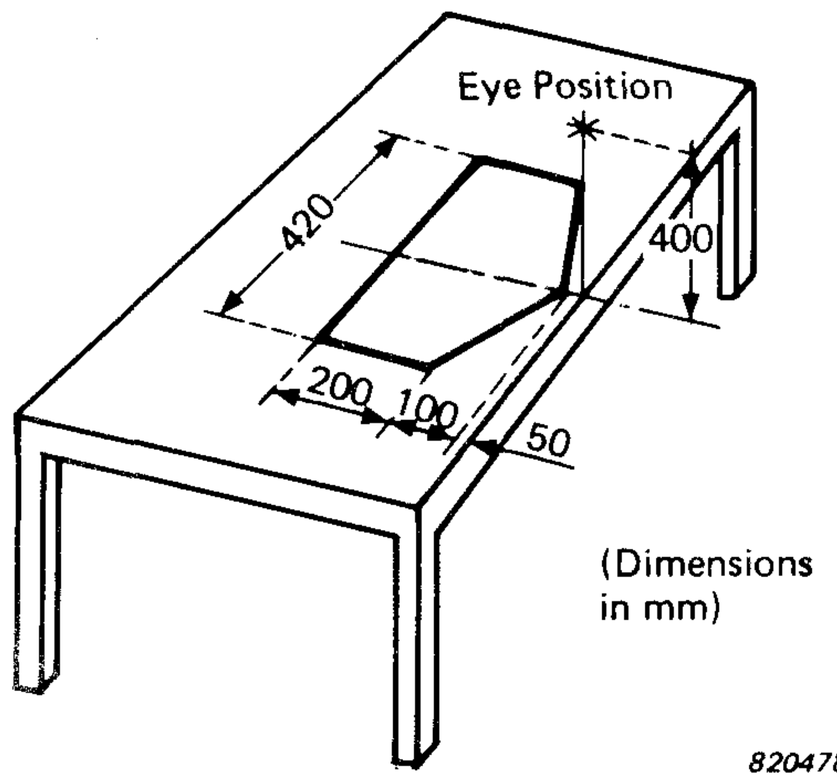

Fig. 3. Field and geometry for evaluating contrast conditions at a desk

techniques are important. Some advice relating to computing techniques for a lighting installation as a whole is given in Section 4.

3. Method for obtaining luminance factors

General discussion of the surfaces and their reflection

Both of the surfaces have a top layer, which is manufactured from a glass material of refractive index, $n = 1{,}55$, and a white ceramic base.

On the light surface, the top layer is printed directly on the base, whereas on the dark surface, a dark material is inserted between the top layer and the base. The dark material is glass containing metal particles with very little reflection, and of the same index of refraction as the top layer. The top layer is for both surfaces given a texture in the form of a smooth relief in a random pattern. The dark surface has the stronger texture of the two. Both surfaces are considered to define plane reflective visual tasks, typically paper with characters. The surfaces show a specular reflection in the top layer.

For a perfectly plane surface the specular reflection follows the geometry of a mirror reflection, i.e. the incident and the reflected rays form the same angle V_i with the normal of the plane. The reflectance , ρ, is a function of V_i given by Fresnel (to be discussed later on).

The texture of the surfaces has the effect that the reflected light is scattered into a certain angular range. This effect can be studied in more detail, **assuming that the textured surface is made up of a large number of small facets of different orientations.** The light surface further shows a relatively strong diffuse reflection, whose distribution is distorted somewhat by the passage of the light both in and out of the top layer. The dark surface shows a similar but much weaker diffuse reflection. Thus the luminance factor of either one of the surfaces, β, is taken to be the sum of the contributions β_s and β_d from the specular and the diffuse reflection, respectively:

$$\beta = \beta_s + \beta_d$$

In the following subsections, the specular reflection is first considered and then the diffuse contribution to the luminance factor.

Fresnel reflection in a planar surface

A planar surface dividing air from glass reflects a part of the incoming luminous flux. The other part is transmitted into the glass. The direction

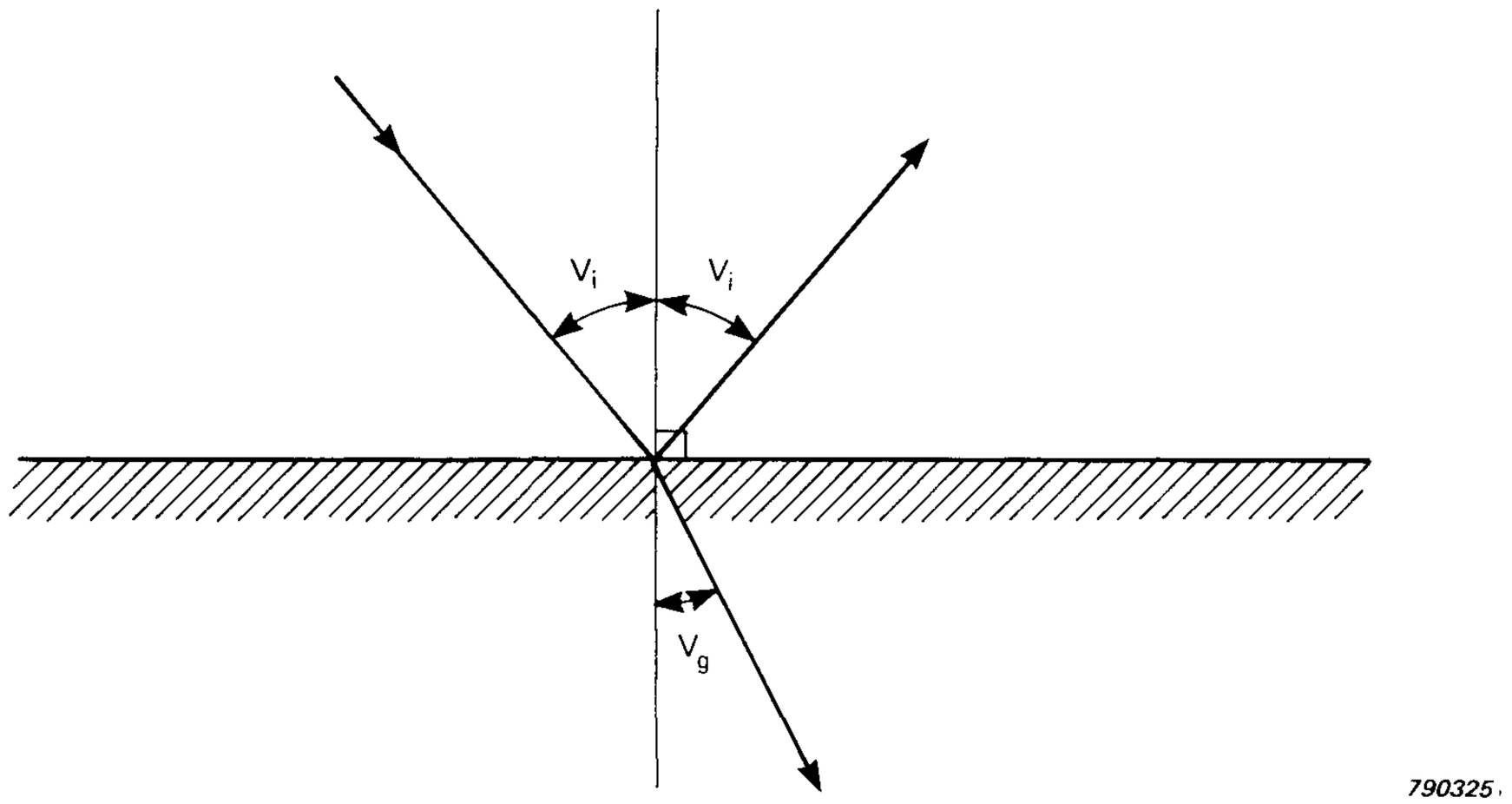

Fig. 4. Angles of reflected and transmitted light

of the reflected light is like the one for mirror reflection in the plane i.e. the incoming and the reflected rays form the same angle, V_i, with the normal to the surface. The transmitted ray forms a smaller angle, V_g, with the normal, as determined by the index of refraction of the glass, n, by (see Fig.4):

$$n = \frac{\sin V_i}{\sin V_g}$$

The fraction of the light reflected in the surface is given by the Fresnel equation for the reflectance assuming non-polarized light:

$$\rho(V_i) = \frac{1}{2}\left(\frac{\sin^2(V_i - V_g)}{\sin^2(V_i + V_g)} + \frac{\tan^2(V_i - V_g)}{\tan^2(V_i + V_g)}\right)$$

The refractive index of the glass of the surfaces is $n = 1{,}55$. The function $\rho(V_i)$ for this value of n is shown in Fig.5. It is observed that the equation for $\rho(V_i)$ applies as well, when the light falls on the surface from the glass.

3.1. An expression for the specular reflection

In a given geometrical situation, only facets of a certain orientation fulfil the condition of mirror reflection. These facets determine β_s for the relevant geometry.

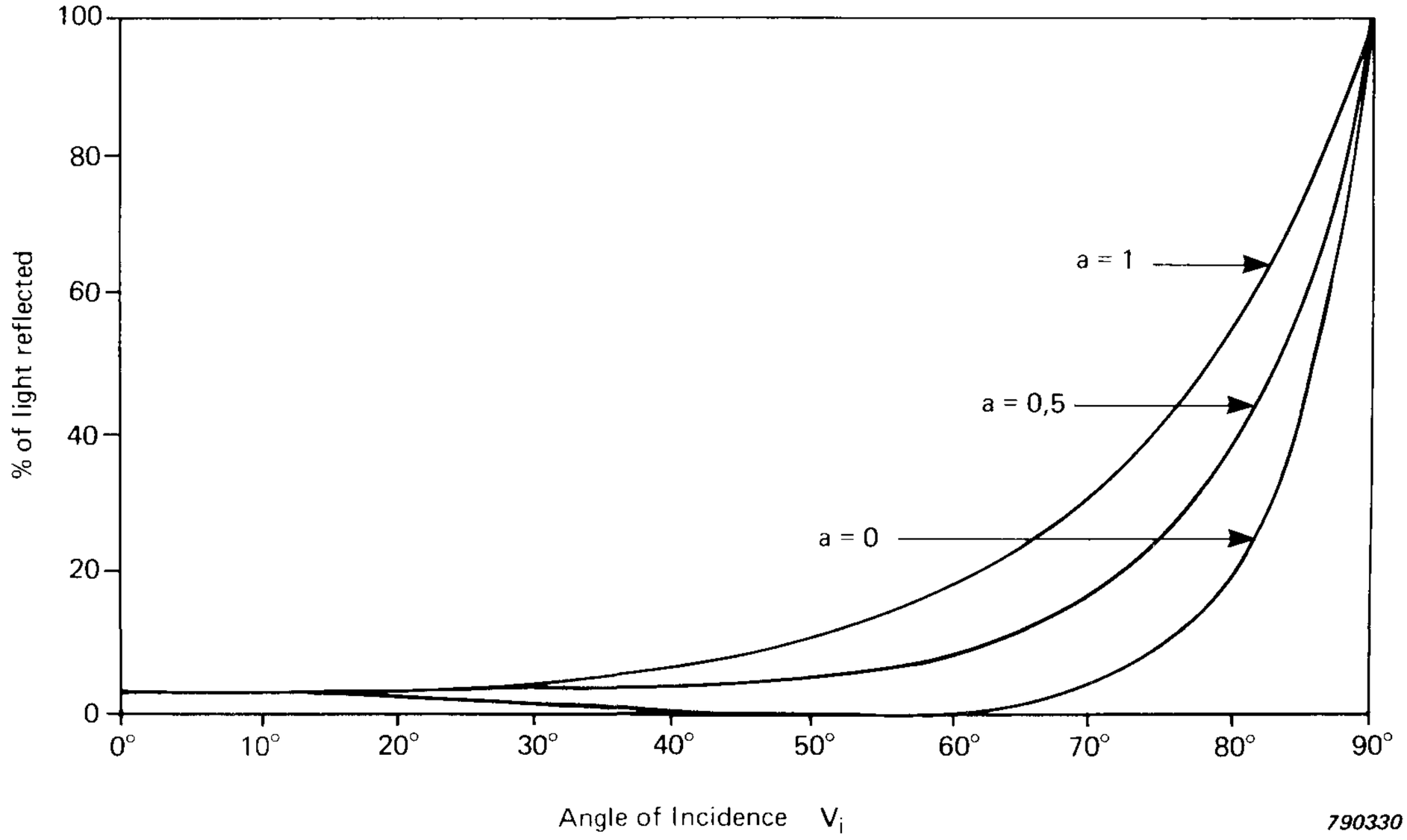

Fig. 5. Reflectance $\rho(V_i)$ for an air-glass surface and refractive index of the glass of 1,55. The middle curve is for non-polarized light

In practice, one has to allow for some spread in the orientation of the reflecting facets, as a meaningless result would otherwise be obtained for β_s. This corresponds to allowing for some variation in the geometrical situation. Thus it is assumed that facets of orientations in a small solid angle, $d\omega$, are reflecting. The area of these facets is dS.

On this assumption, the reflected light is found in another, small solid angle given by:

$$d\omega' = 4 \cdot \cos V_i \cdot d\omega \qquad \text{(ref.4)}$$

A fraction $\rho(V_i)$ of the luminous flux $d\phi$ falling on dS is reflected. The intensity of the reflected light is:

$$I = \frac{\rho(V_i) \cdot d\phi}{d\omega'} = \frac{\rho(V_i) \cdot d\phi}{4 \cdot \cos V_i \cdot d\omega}$$

The average luminance of the area A of the surface as measured in its plane is:

$$L = \frac{I}{A \cdot \cos V_A} = \frac{\rho(V_i) \cdot d\phi}{4 \cdot \cos V_i \cdot d\omega \cdot A \cdot \cos V_A}$$

The illuminance E' on the facet plane expressed by the illuminance E on the surface plane, must be:

$$E' = E \cdot \cos V_i / \cos V_C \qquad \text{(see Fig.6)}$$

Also

$$E' = \frac{d\phi}{dS}$$

Thus

$$E = \frac{d\phi \cdot \cos V_C}{dS \cdot \cos V_i}$$

Finally the luminance factor is obtained:

$$\beta_s = \frac{\pi \cdot L}{E} = \left(\frac{\pi \cdot \rho(V_i)}{4 \cdot \cos V_A \cdot \cos V_C} \right) \cdot \left(\frac{dS}{A \cdot d\omega} \right)$$

The surface texture enters into this expression by means of the last term, which is the area of facets, *dS*, with orientations within the solid angle, $d\omega$, in proportion to that solid angle and in proportion to the area of the standard, *A*. This term is called the surface roughness factor, *f*, and obviously is a function of the orientation.

The orientation of a facet must in principle be given by two angles, one of which is the angle of tilt, V_n, see Fig.6. The other angle could relate to the rotation of the facet about the normal of the surface. However, due to the randomness of the surface texture, the distribution *f* is considered to be a function of V_n only. Thus:

$$\beta_s = \frac{\pi \cdot \rho(V_i) \cdot f(V_n)}{4 \cdot \cos V_A \cdot \cos V_C}$$

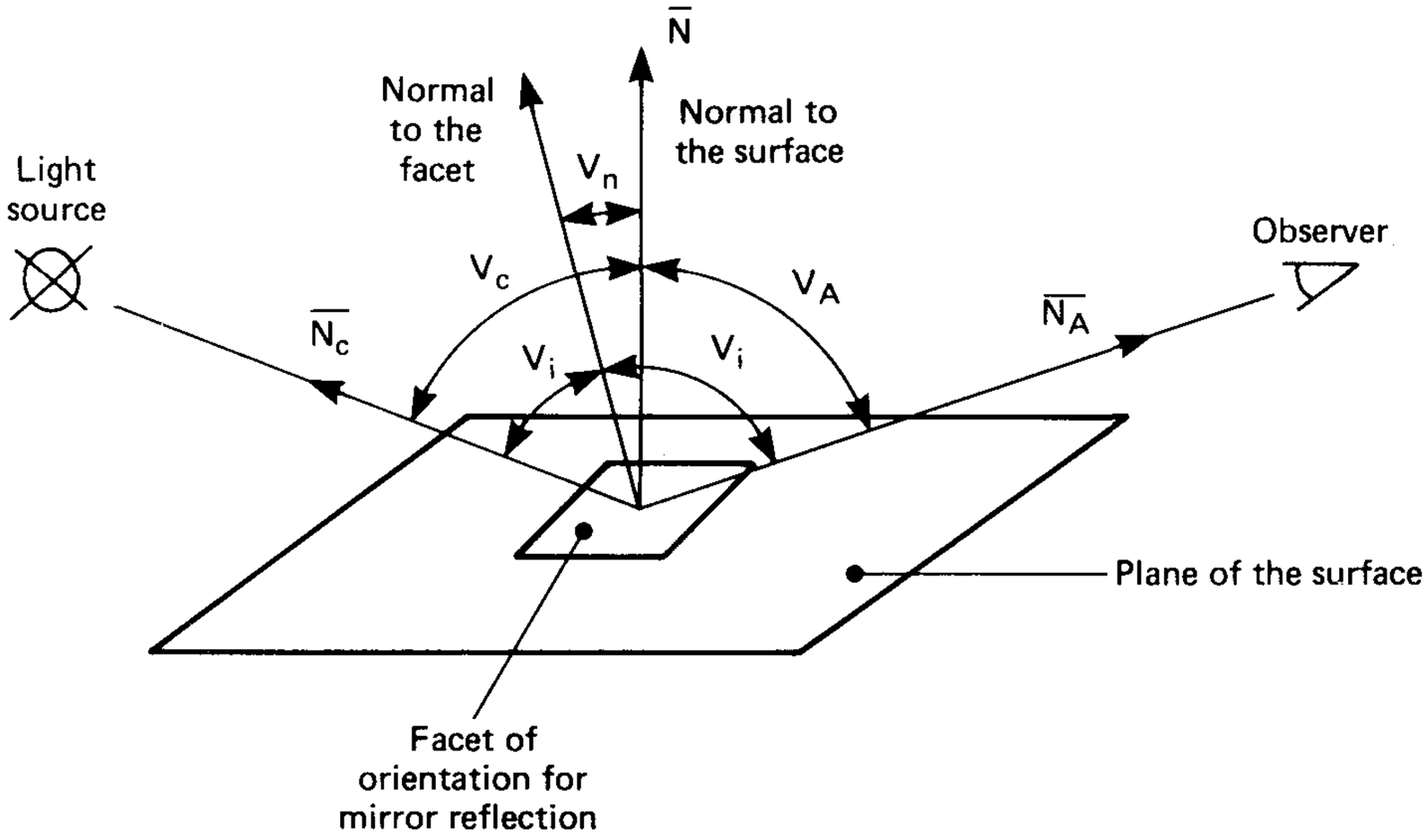

Fig. 6. The geometry of illumination and observation can in general be specified by the following unit vectors:
$\overline{N}$, normal to the plane of the standard
$\overline{N}_A$, points from the standard to the observer
$\overline{N}_C$, points from the standard to the light source

In the expression for the luminance factor the cosines of the viewing angle, V_A, of the angle of incidence on the standard, V_C, and for the angle of incidence on those facets of the correct orientation for mirror reflection, V_i, are used. Further the angle of tilt of those facets, V_n, is used. These values are found by:

$$\cos V_A = \overline{N} \cdot \overline{N}_A \qquad \cos V_C = \overline{N} \cdot \overline{N}_C$$

$$\cos V_i = {}^1/_2 \, | \, \overline{N}_A + \overline{N}_C \, |$$

$$\cos V_n = {}^1/_2 (\cos V_A + \cos V_C) / \cos V_i$$

In principle, the expression for β_s is accurate only for such geometries where the reflecting parts are both visible and illuminated. It is seen later, however, that facets of a large inclination are very few, so that the effects of shadows should be negligible. Thus, it is possible to account for the data of the reflection tables without making corrections for shadows. The various terms in the expression indicate that the luminance factor varies strongly with the geometry. The term $f(V_n)$ is, however, not judged easily in this sense, and is therefore discussed shortly below.

The integral of $f(V_n)$ over all possible orientations equals of course the total surface of the facets, S, divided by the area, A, of the standard as measured in the plane.

This ratio is somewhat larger than unity due to the tilt of the facets:

$$\int_0^{2\pi} f(V_n)\, d\omega = S/A \geqslant 1$$

The integral can be performed using

$$d\omega = 2\pi \sin V_n \cdot dV_n$$

thus

$$2\pi \cdot \int_0^{\pi/2} f(V_n) \sin V_n \cdot dV_n = S/A \geqslant 1$$

For a perfectly plane surface, $f(V_n)$ is a peak function situated at $V_n = 0°$. For another simple surface, the upper part of a sphere, $f(V_n)$ is constant up to a certain value of V_n, where it drops sharply to zero. The actual surfaces lie somewhere in between the two above-mentioned extremes. At $V_n = 0°$, $f(V_n)$ is very large, but decreases rapidly with V_n (see Table 3).

Thus the luminance factor is high, when the direction of observation is close to the direction obtained by mirror reflection of the illumination in the plane of the standard.

3.2. An expression for the diffuse reflection

The base of the light standard is assumed to reflect diffusely with a luminance factor, β_0. The luminance factor for the diffuse reflection of the surfaces is given by β_0, and by the losses in the top layer for both the incident and the reflected light. Absorption in the top layer is ignored, so that only losses by reflection in the top layer need to be considered.

These losses were easily accounted for by Fresnel reflection, had the surface been plane. It is seen later that by far the most of the surface is tilted less than 10°. Further, the Fresnel reflection is small and relatively constant up to approx. 60°. Thus, for the transmittance from the base to

$$\beta = \frac{R \cdot F}{\cos V_A \cdot \cos V_C} + G \cdot \beta'$$

$V_A \leqslant 45°$ $V_C \leqslant 80°$

$\cos V_i$	R
0	
0,05	
0,10	
0,15	
0,20	
0,25	
0,30	
0,35	
0,40	
0,45	0,1164
0,50	0,0973
0,55	0,0829
0,60	0,0721
0,65	0,0640
0,70	0,0580
0,75	0,0537
0,80	0,0507
0,85	0,0487
0,90	0,0474
0,95	0,0467
1,00	0,0465

$\cos V_C$	G
0	
0,05	
0,10	
0,15	0,622
0,20	0,699
0,25	0,756
0,30	0,798
0,35	0,834
0,40	0,859
0,45	0,884
0,50	0,903
0,55	0,917
0,60	0,928
0,65	0,936
0,70	0,942
0,75	0,946
0,80	0,949
0,85	0,951
0,90	0,953
0,95	0,953
1,00	0,954

light st.: β' = 0,76
dark st.: β' = 0,014

V_n	F	
	light st.	dark st.
0°	21,2	41,2
1°	20,2	38,2
2°	18,06	29,6
3°	14,77	20,9
4°	11,78	13,43
5°	9,03	9,27
6°	6,71	5,85
7°	5,20	4,06
8°	3,65	2,69
9°	2,84	2,02
10°	2,29	1,469
11°	1,783	1,115
12°	1,312	0,809
13°	1,045	0,605
14°	0,903	0,479
15°	0,762	0,377
16°	0,652	0,283
17°	0,573	0,212
18°	0,503	0,165
19°	0,448	0,134
20°	0,401	0,110
21°	0,361	0,094
22°	0,322	0,079
23°	0,291	0,079
24°	0,259	0,071
25°	0,236	0,071
26°	0,212	0,063
27°	0,188	0,063
28°	0,173	0,055
29°	0,157	0,055
30°	0,141	0,047
31°	0,134	0,047
32°	0,126	0,039
33°	0,118	0,039
34°	0,110	0,031
35°	0,102	0,031
36°	0,094	0,024
37°	0,086	0,024
38°	0,079	0,016
39°	0,071	0,016
40°	0,063	0,008
41°	0,055	0,008
42°	0,047	0
43°	0,039	0
44°	0,031	0
45°	0,024	0
46°	0,016	0
47°	0,008	0
48°	0	0
49°	0	0
50°	0	0

840435

Table. 3. Expression and tabulated data for the calculation of luminance factors, β, for the light and the dark reflectance surfaces

the observer for which the relevant angular range is limited to $V_A \leqslant 45°$, the situation is simple. The surface can be assumed to be plane, and the transmittance from the base to the air can even be given to a good approximation by the figure 0,95.

For the transmittance of the luminous flux from the light source to the base, the interesting range goes as high as 80°. It is therefore necessary to take into account the variation of the Fresnel reflection, and even to apply a correction factor $g(V_C)$ at the largest angles in the range. The correction factor is to be larger than unity, as facets tilted towards the direction of illumination have simultaneously a relatively high illuminance and a relatively high transmittance, (see Table 3).

The total expression for β_d is thus:

$$\beta_d = 0.95 \cdot \beta_0 \cdot (1-\rho(V_C)) \cdot g(V_C)$$

This expression is also used to account for the weak diffuse reflection of the dark surface. It is observed that interreflection between the white base and the upper surface adds a small and fixed amount to β. This can be taken into account by adjusting the value of β_0.

3.3. Method for computing luminance factors

Combining the expressions for β_s and β_d we have:

$$\beta = \beta_s + \beta_d = \frac{\pi}{4} \cdot \frac{\rho(V_i)}{\cos V_A \cdot \cos V_C} \cdot f(V_n) + (1-\rho(V_C)) \cdot \beta_0 \cdot 0{,}95$$

The free parameters of this expression are the function $f(V_n)$, the value β_0 (very small for the dark surface) and the correction function $g(V_C)$.

These parameters have been determined in a procedure involving partly trial and error and partly regression techniques.

A further regrouping of the data is shown below:

$$\beta = \frac{R \cdot F}{\cos V_A \cdot \cos V_C} + G \cdot \beta'$$

where $R = \rho(V_i)$

$$F = \frac{\pi}{4} \cdot f(V_n)$$

$$G = (1 - \rho(V_C)) \cdot g(V_C)$$

$$\beta' = \beta_0 \cdot 0.95$$

F and β' will depend on which of the two surfaces is considered.

Table 3 contains the values of F in steps of 1° for both surfaces. It further contains the values of β' and a tabulation of the Fresnel reflectance, R. The Fresnel reflectance is included, as the equation is somewhat cumbersome. The variable used is $\cos V_i$ instead of V_i, as the use of the inverse cosine function is thereby avoided, and a more convenient tabulation is obtained.

Finally Table 3 contains a tabulation of the function G. Again the cosine is used for the same reason as for using $\cos V_i$. The correction factor $g(V_C)$, included in G, is not shown independently in Table 3. The factor is only different from 1 for 5 (defined) values of $\cos(V_C)$:

$\cos V_C$	$g(V_C)$
0.15	1.12
0.20	1.07
0.25	1.04
0.30	1.02
0.35	1.01

The result of calculating the luminance factors by this method is in agreement with the measured values of Tables 1 and 2. The agreement can be judged from Table 4 showing the difference between **contrast** values obtained from measured and from calculated luminance factors. Table 4 shows that deviations in contrasts in almost all cases are smaller than 0,02 for single directions of illumination. In practical situations, the deviations will mostly be smaller. It is concluded that calculations of contrasts can safely be based on the method of Table 3.

The method has been designed to work fast by a computer, e.g. by using mainly cosines of angles instead of the angles themselves. A general method of obtaining the angles is given in Fig.6. The method of Fig.6

	V_B \ V_C	0	3	5	7	10	15	20	25	30	35	40	45	50	60	70	80
	0	−0,02	−0,02	−0,01	0,00	0,02	0,01	0,01	0,00	0,00	0,00	0,00	0,00	0,00	0,00	0,00	0,00
	5	−0,02	−0,02	0,00	−0,01	0,02	0,01	0,01	0,00	0,00	0,00	0,00	0,00	0,00	0,00	0,00	0,00
	10	−0,02	−0,02	0,00	−0,01	0,00	0,01	0,00	0,00	0,00	0,00	0,00	0,00	0,00	0,00	0,00	0,00
V_A	20	−0,02	−0,01	0,00	0,01	0,01	0,02	0,10	0,00	0,00	0,00	0,00	0,00	0,00	0,00	0,00	0,00
=5°	50	−0,02	−0,02	0,00	0,01	0,03	0,01	0,00	0,00	0,00	0,00	0,00	0,00	0,00	0,00	0,00	0,00
	90	−0,02	−0,02	0,00	0,00	0,00	0,00	0,00	0,00	0,00	0,00	0,00	0,00	0,00	0,00	0,00	0,00
	120	−0,02	−0,03	−0,03	−0,02	0,00	0,00	−0,01	0,00	0,00	0,00	0,00	0,00	0,00	0,00	0,00	0,00
	180	−0,02	−0,01	−0,03	−0,01	−0,01	0,00	0,00	0,00	0,00	0,00	0,00	0,00	−0,01	0,00	0,00	0,01

841461

	V_B \ V_C	0	5	10	15	20	23	25	27	30	35	40	45	50	60	70	80
	0	0,00	0,00	−0,01	0,02	0,02	−0,01	−0,02	−0,02	0,00	0,00	0,00	0,00	0,00	0,01	0,01	−0,02
	5	0,00	0,00	0,01	0,02	0,02	0,01	−0,02	0,00	−0,01	−0,01	0,00	0,00	0,00	0,01	0,01	−0,02
	10	0,00	0,00	0,01	0,02	0,02	0,01	0,01	0,00	0,00	0,00	0,00	0,00	0,00	0,01	0,01	−0,01
V_A	20	0,00	0,00	0,01	0,02	0,02	0,01	0,01	0,00	0,01	0,00	0,00	0,01	0,00	0,01	0,01	−0,01
=25°	50	0,00	0,00	0,00	0,00	0,00	0,00	0,00	0,00	0,00	0,00	0,00	0,00	0,00	0,00	0,00	−0,01
	90	0,00	0,00	0,00	0,00	0,00	0,00	0,00	0,00	0,00	0,00	0,00	0,00	−0,01	0,00	0,00	0,00
	120	0,00	0,00	0,00	0,00	0,00	0,00	0,00	0,00	0,00	0,00	−0,01	−0,01	0,00	0,00	0,00	0,00
	180	0,00	0,00	0,00	0,00	0,00	0,00	0,00	0,00	0,00	0,00	−0,01	−0,01	0,00	0,00	0,00	0,00

841462

	V_B \ V_C	0	10	15	20	25	30	35	40	43	45	47	50	55	60	70	80
	0	0,00	0,00	0,00	0,00	0,00	0,01	0,02	0,03	0,03	0,05	0,01	0,00	−0,01	−0,01	0,00	0,02
	5	0,00	0,00	0,00	0,00	0,00	0,01	0,00	0,01	0,01	−0,01	−0,01	0,00	−0,01	0,00	0,00	0,02
	10	0,00	0,00	0,00	0,00	0,00	0,01	0,00	0,00	0,01	0,00	−0,01	0,01	0,00	0,00	0,01	0,02
V_A	20	0,00	0,00	0,00	0,00	0,01	0,00	0,00	0,00	0,00	0,00	0,00	0,00	0,01	0,01	0,02	0,00
=45°	50	0,00	0,00	0,00	0,00	0,00	0,00	0,00	0,00	0,00	0,00	0,00	0,00	0,00	0,00	0,00	0,01
	90	0,00	0,00	0,00	0,00	0,00	0,00	0,00	0,00	0,00	0,00	0,00	0,00	0,00	0,00	0,00	0,01
	120	0,00	0,00	0,00	−0,01	0,00	0,00	0,00	0,00	0,00	0,00	0,00	0,00	0,00	0,00	0,00	0,00
	180	0,00	−0,01	−0,01	0,00	−0,01	0,00	0,00	0,00	0,00	0,00	0,00	0,00	0,00	0,00	0,00	0,00

841463

Table. 4. Difference between contrast values obtained from measured and from calculated luminance factors

relates to the situation, where the geometry is described by vectors. In cases where the geometry is described by the angles V_A, V_B and V_C of Fig.2, the following vectors can be used:

$$\overline{N}_A : (\sin V_A, \quad 0, \quad \cos V_A)$$

$$\overline{N}_C : (-\cos V_B \cdot \sin V_C, \quad -\sin V_B \cdot \sin V_C, \quad \cos V_C)$$

$$\overline{N} : (0, \quad 0, \quad 1)$$

4. Some advice concerning computing techniques

Some advice concerning computing techniques can be drawn from the fact that the half-width of the specular peak of the dark surface is about ± 6°. Thus at the height of the observation point of 40 cm above the field, the field has to be searched with a grid of approximately 6 cm in order just to locate a specular reflection. A finer grid of 3 or 1 1/2 cm is required in order to determine the minimum *CRF* to a good accuracy. In

order to keep the computing time down, it is probably worthwhile to combine those two grids. First the *CRF* can be computed for the coarse 6 cm grid, and next the *CRF* can be computed for those points in the finer grid, which are neighbours to points of a low *CRF*.

Similarly, luminaires have to be subdivided into parts, which do not subtend more than the above mentioned $\pm 6°$, as seen from the point in the grid. At a luminaire mounting height of say 1,5 m above the working field, the dimensions of such parts are approximately 0,3 m. Thus luminaires for fluorescent tubes generally have to be subdivided into parts along their longitudinal axis, and in some cases also along the other axis.

A similar subdivision is in principle required also for the ceiling and the walls in a room. As a first approximation one could, however, assume that the luminance of the ceiling and walls is uniform. This is the reference situation which tends to give a *CRF* of the indirect lighting equal to unity.

The *CRF's* of the direct and indirect components of lighting can be added in the proportions to which they contribute to the luminance of the light surface of the contrast standard. As a further approximation the proportions can be replaced by the proportions of the illuminances:

$$CRF \approx \frac{CRF_d \cdot E_d + CRF_i \cdot E_i}{E_d + E_i}$$

where CRF_d and CRF_i are the *CRFs* in the direct and the indirect illumination, respectively. E_d and E_i are the illuminances of these illuminations.

A more precise calculation can be obtained from:

$$CRF = \frac{CRF_d \cdot L_d + CRF_i \cdot L_i}{L_d + L_i}$$

where the L's are luminances of the white standard surface. The formula as such applies exactly, and the L_d is known from the CRF_d calculation. But the L_i must be estimated from E_i. For this purpose the average luminance factor of 0,74 for the light surface might be used. Thus $L_i = 0{,}74 \cdot E_i/\pi$.

In most cases the diffuse contribution is quite small, but at the borders and especially at the corners of the room, the diffuse contribution is significant.

References

[1] LYNES, J.A., *"Designing for Contrast Rendition"*, Ltg. Res. & Technol, Vol.14, No. 1, 1982

[2] FISCHER, D., *"Suitable Quality Classes for the Contrast Rendering Factor"*, CIE-Journal, Vol.1, 1982

[3] YDE, L. & NIELSEN,O., *"Reflection Standard, Make and Characteristics"*, Proceedings of the CIE No. 314, 1979

[4] RENSE, W.A. Jnl. Opt. Soc. Amer. 40. 56, 1950

[5] CUTTLE, K., IES Lighting Rev. (Australia)s", 119, October 1979

PROPER USE OF WEIGHTING FUNCTIONS FOR IMPACT TESTING*

by

Richard C. Sohaney
and
James M. Nieters

ABSTRACT

Force and exponential windows are commonly used to weight the time signals when impact methods are used for structural dynamics testing. In modern signal processing instrumentation, these windows can be selected and adjusted by the user. Improper application of the window can result in measurement errors. This paper discusses how to evaluate the force and response signals to determine the proper type and amount of weighting to apply. The effects of signal conditioning on the shape of the force pulse are described. A method of evaluating the signal noise floor in order to determine an optimal amount of exponential weighting is presented.

SOMMAIRE

Des fenêtres exponentielles et de force sont couramment utilisées pour pondérer les signaux temporels, lorsque l'on effectue des essais dynamiques de structures par des méthodes d'impact. Dans les appareils modernes de traitement du signal, ces fenêtres peuvent être choisies et réglées par l'utilisateur même. Une utilisation incorrecte de ces fenêtres peut se traduire par des erreurs de mesure. Cet article traite de l'évaluation des signaux de force et de réponse, afin de déterminer le type et la quantité de pondération à appliquer. Les effets du conditionnement du signal sur l'allure de l'impulsion de force sont décrits, et une méthode d'évaluation du seuil de bruit du signal permettant de déterminer la quantité optimale de pondération exponentielle est présentée.

---

* Printed in the Proceedings of the Third International Modal Analysis Conference, Orlando, Florida, USA 1985

ZUSAMMENFASSUNG
Bei dynamischen Untersuchungen an mechanischen Strukturen mit Impulsmethoden werden für die Zeitsignalbewertung meist Fenster für das Erregersignal und exponentielle Fenster für das Antwortsignal verwendet. Mit modernen Signalanalysatoren lassen sich diese Bewertungsfenster frei wählen und einstellen, was bei unsachgemäßer Anwendung zu Meßfehlern führen kann. Im folgenden wird darauf eingegangen, wie Erregungs- und Antwortsignale zu beurteilen sind, um dadurch die richtige Art und Größe des Zeitfensters festzulegen. Außerdem sind die Einflüsse der Signalaufbereitung auf die Form des Erregerimpulses beschrieben. Der Aufsatz befaßt sich auch mit einer Methode zur Beurteilung von Fremdsignalen, um die optimale Größe der exponentiellen Bewertung zu bestimmen.

Introduction

Two signal processing problems inherent in impact testing are noise and leakage. Noise can be a problem in both the force and response signals and is mainly a consequence of a long analyzer time record. Leakage is of most concern in the response signal and is a consequence of too short a time record. These two problems may occur separately or together depending on the structure under test, the frequency range of the test, and the analyzer transform size.

Special force and exponential windows have been developed for impact testing to reduce noise and leakage [1]. This paper discusses proper application of these windows while pointing out common errors. Guidelines are developed for setting the width of the force window and selecting the decay rate of the exponential window. Alternative impact testing methods and windows are presented for measurement situations where the analyzer time record length is very long. Good measurement technique is emphasized throughout.

Windowing the force signal

The purpose of the force window is to improve the signal to noise ratio in the force signal. Typically, the force pulse has a low rms energy level even though its peak level may be high. Also, the pulse duration is short compared to the analyzer time record length. Noise can be a problem because the total energy of noise in the time record can be significant compared to the energy in the pulse.

The general form of the force window is shown in Fig.1. It consists of a rectangle of unity amplitude with leading and trailing half cosine tapers to zero. Unity amplitude preserves the pulse portion of the signal while zero eliminates noise. The tapers smooth the data to zero at the ends of the window to avoid artificial sharp transitions in the time signal.

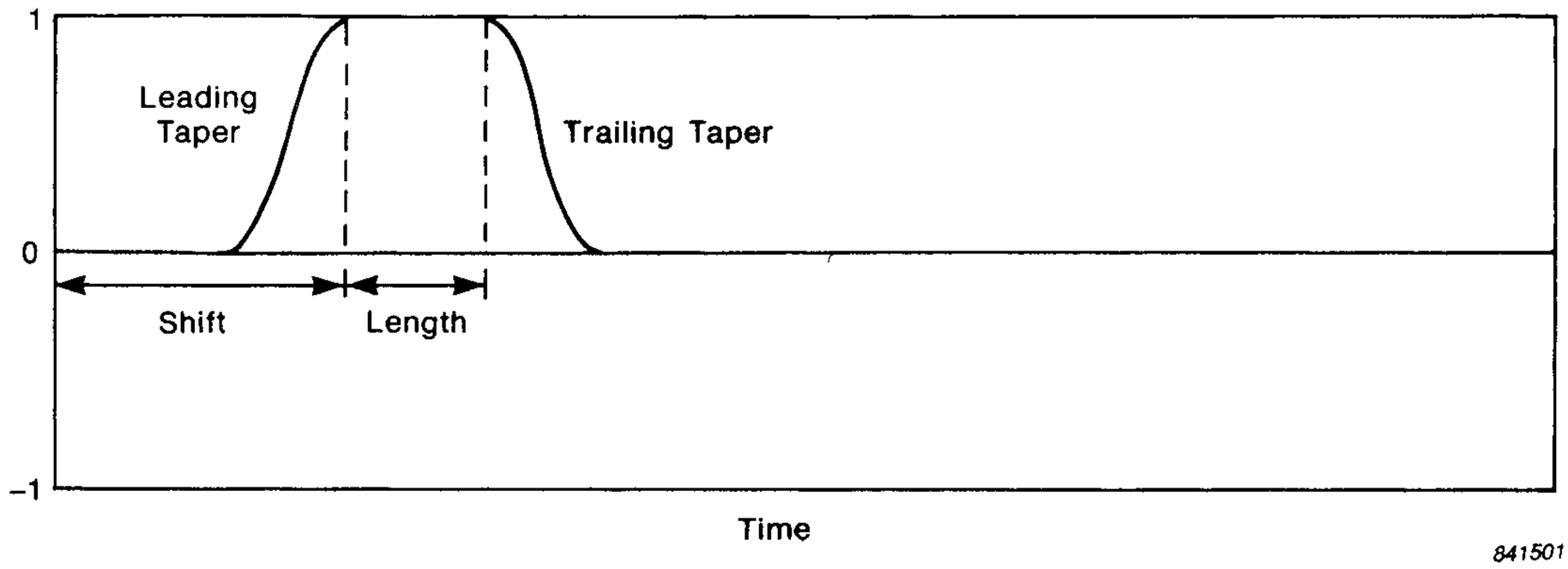

Fig. 1. General form of force window

Fig.2 shows a typical force pulse obtained from an impact hammer. The pulse consists of an initial sharp positive peak followed by decaying oscillations referred to as ringing. Note in particular the ringing. A common error is to attribute the ringing to "hammer ringing" or "transducer ringing" and eliminate it using the force window [2]. Actually, the ringing is part of the force pulse and is a consequence of the anti-aliasing filter in the analyzer used to measure the force signal.

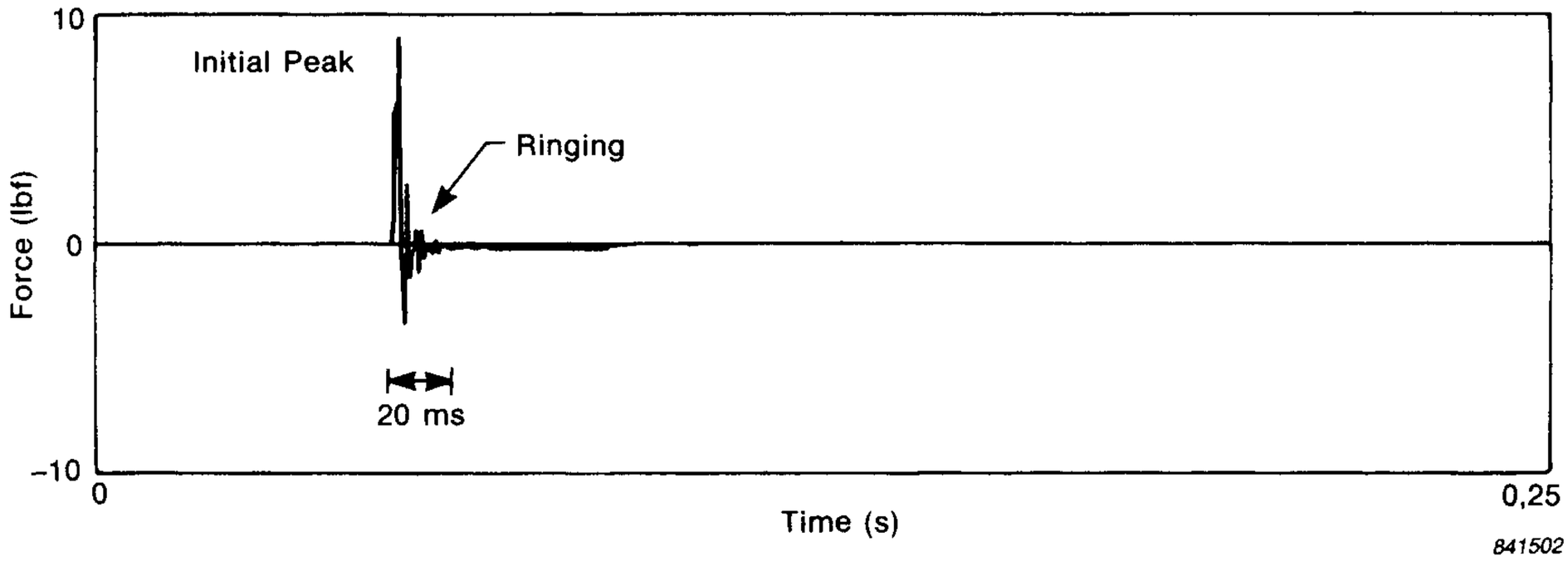

Fig. 2. Typical force pulse measured with analyzer full scale frequency 800 Hz

To demonstrate the origin of ringing, the force pulse can be examined with the analyzer set to its highest frequency range and the low pass anti-aliasing filters turned off.* Fig.3(a) shows a force pulse measured with the analyzer in this mode. Note that the pulse shape is well defined, smooth, and there is no ringing.

---

* Examining the force pulse in this manner should normally be performed at the initial stages of an impact test as recommended by Corelli and Brown [2]. The force pulse should be inspected for clipping indicating amplifier overload somewhere in the measurement chain.

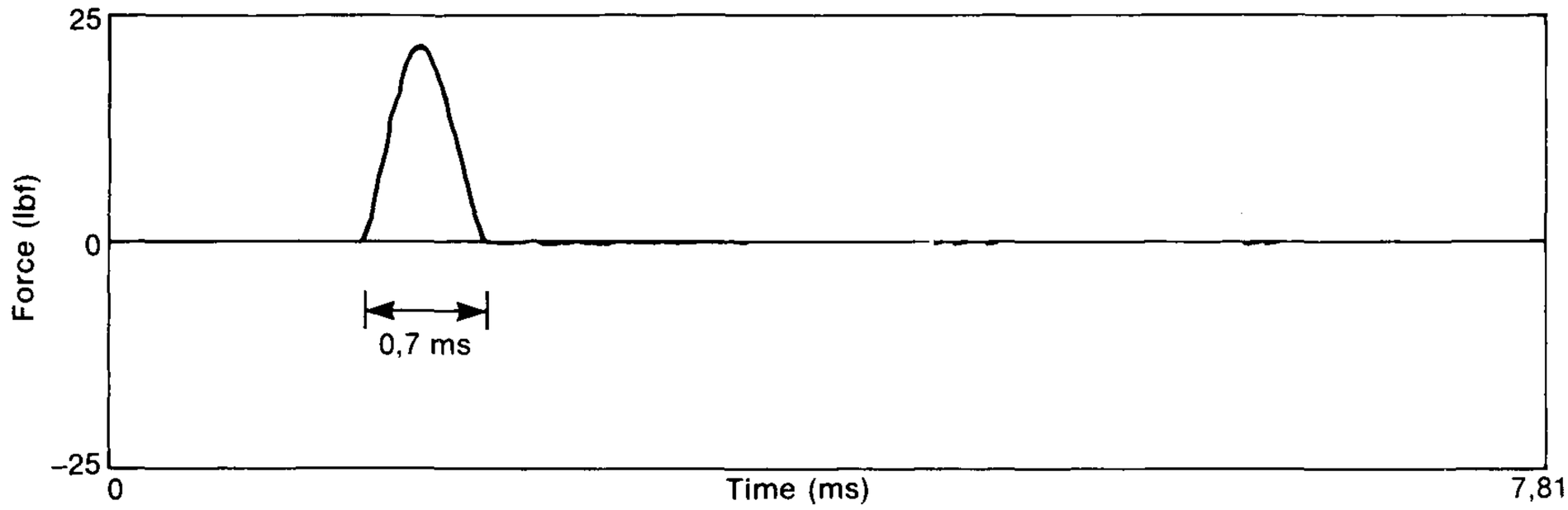

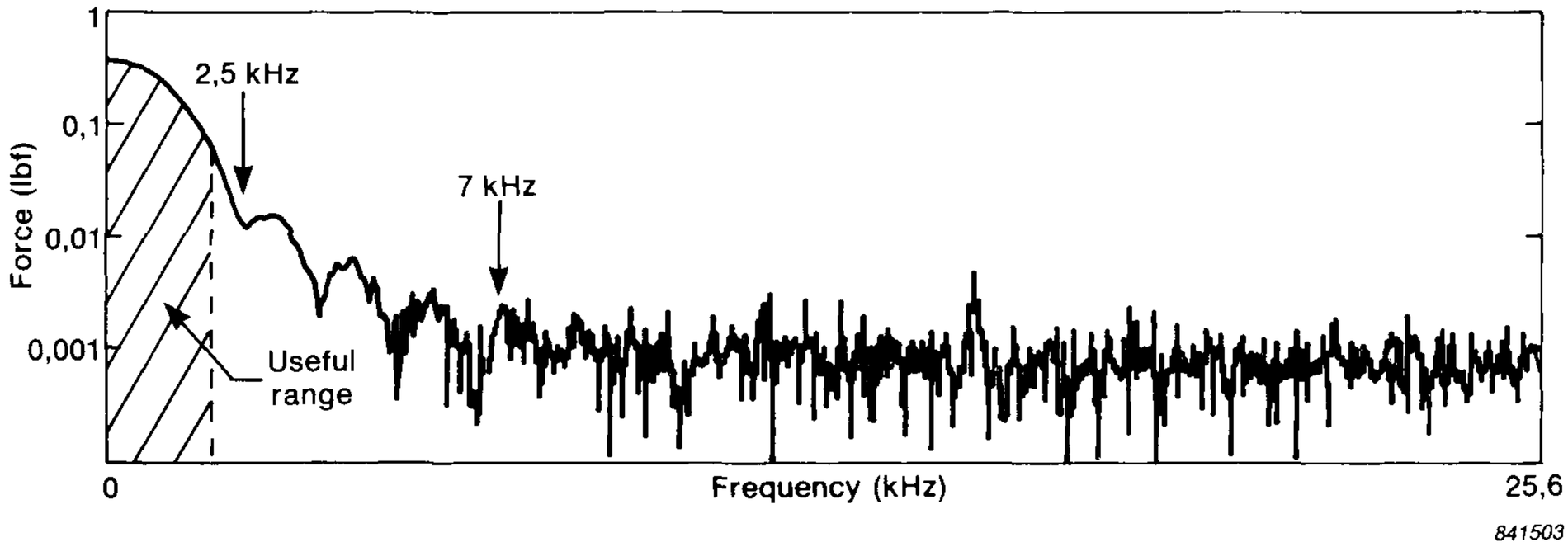

841503

Fig. 3. a) Force pulse measured with analyzer full scale frequency at 25.6 kHz and anti-aliasing filters off
b) Spectrum of the force pulse

The spectrum of this pulse is shown in Fig.3(b). This spectrum exhibits the characteristic form of pulse spectra; a series of decreasing amplitude lobes separated by zeroes in the spectrum. Typically, the first zero occurs at a frequency 1,8 to 2,0 times the reciprocal of the pulse duration. Above 7 kHz the pulse in Fig.3(a) has little spectral content and the spectrum is dominated by noise. Thus, the pulse has been measured with an analyzer bandwidth (25,6 kHz) wider than the pulse bandwidth (7 kHz). Measured under this condition, ringing is not observed in the force signal.

When the analyzer is set to the desired frequency range of the modal test, a low pass anti-aliasing filter or zoom filter is introduced in each channel. The modal test frequency range is set within the useful frequency range of the force pulse which is well below the frequency of the first zero. Now, the analyzer bandwidth is narrower than the bandwidth of the force pulse. Measured under this condition, ringing is observed in the force signal.

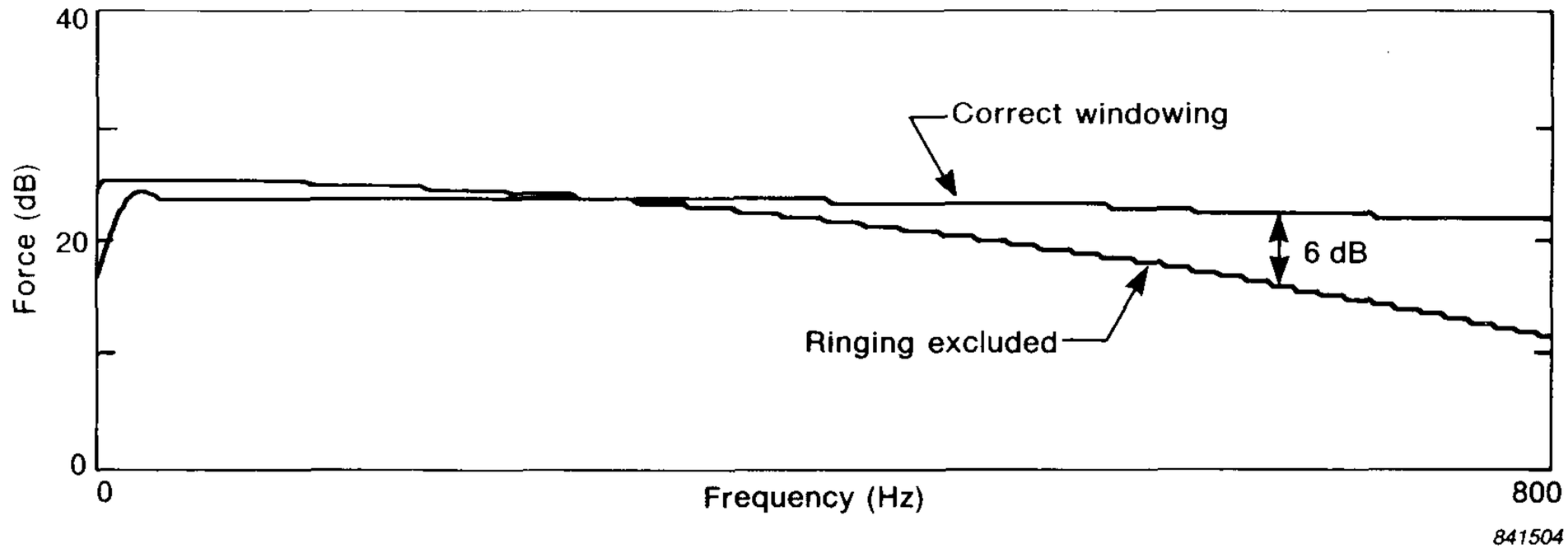

Fig. 4. Force spectrum with correct and incorrect windowing

Filter ringing is not a spurious or false signal. The pulse in Fig.2 is equivalent to the pulse in Fig.3(a), but with its high frequency content filtered out. Alternatively, ringing can be interpreted as energy delayed by the filter. As much as 10% of the energy of the pulse can be contained in the ringing portion. This is energy which is imparted to the structure under test and, therefore, should be included under the force window. Fig.4 compares the force spectrum with and without the ringing included under the window. The error can be as large as 6 dB (50%) at high frequencies.

The duration of the ringing is a function of the filter cut-off frequency and filter slope. Typical anti-aliasing filters built-in commercially available digital frequency analyzers have slopes on the order of 120 dB/octave. These ring for approximately 16/F seconds where F is the filter cut-off in Hz.

Usually, the filter cut off coincides with the analyzer full scale frequency. Common analyzers which display 400 or 800 frequency lines use a sampling frequency 2,56 times the full scale frequency. For these analyzers, the ringing duration in terms of number of samples is approximately 40 (16 multiplied by 2,56), independent of the analyzer frequency range.

A good rule of thumb, then, is to use a force window which extends about 40 times samples past the initial sharp peak of the pulse. The leading edge of the window should be shifted to compensate for any pre-trigger delay in the measurement. A suitable length for the tapers is also 40 samples. A force window set in this manner includes the entire force pulse and optimally rejects noise before and after the pulse.

Windowing the response signal

The response of a structure to an impact is assumed to be a sum of exponentially decaying sinusoids. If the structural response measured by the analyzer has not decayed to zero by the end of the analyzers time record then the measurement is a truncated version of the complete response. A sharp truncation of the time signal will produce leakage error in the estimated frequency response function. The purpose of the exponential window is to add extra decay and artificially force the response to zero and avoid truncation error.

Fig.5 shows the general form of the exponential window. It consists of a leading half cosine taper to unity, followed by an exponential decay with decay constant τ. In order to determine a suitable decay constant for the window, the response signal level at the end of the time record should be evaluated.

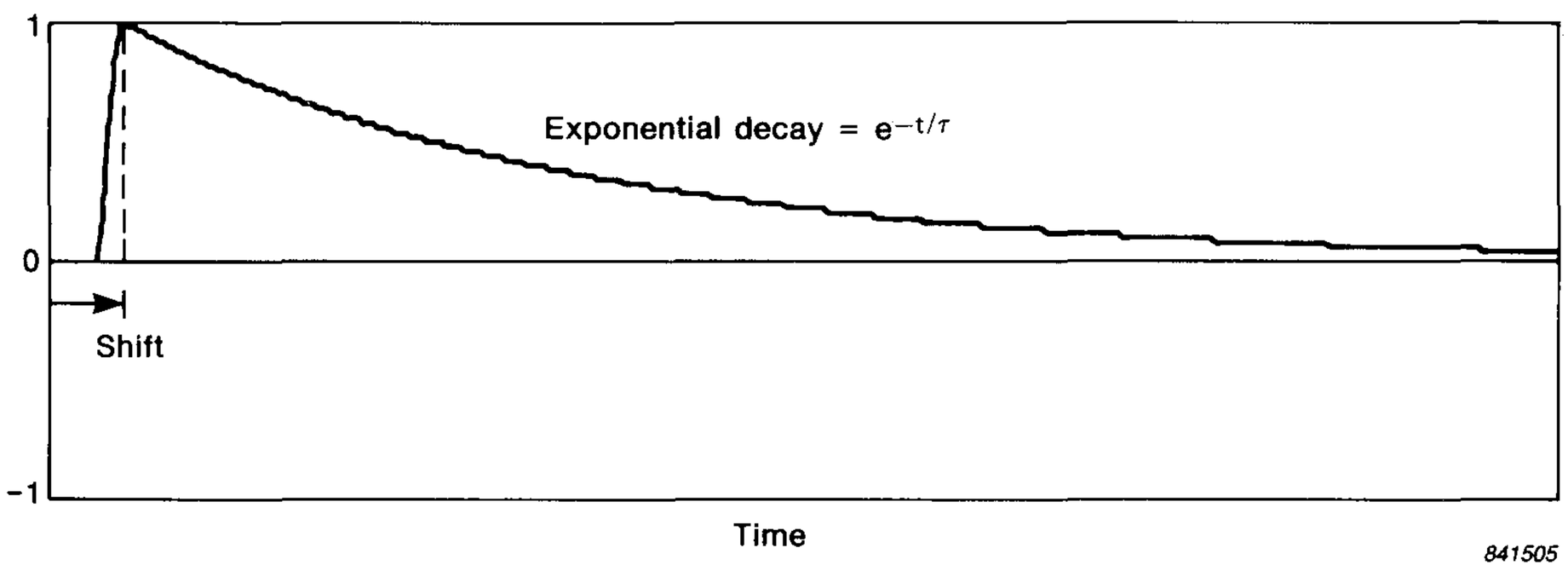

Fig. 5. Exponential window with decay rate τ

Fig.6(a) shows a typical response signal obtained from testing a lightly damped structure. A more convenient way to display the response signal is to use the magnitude function obtained using the Hilbert Transform*. The magnitude function represents the positive envelope of the response signal and can be displayed using a logarithmic vertical axis as in Fig.6(b). An exponential decay on a logarithmic vertical scale is a straight line with negative slope. Furthermore, a logarithmic vertical axis allows the peak signal level and the noise floor to be visible in the same display. It is easy to observe in Fig.6(b) that the response has decayed 30 dB by the end of the time record. Also, the signal noise floor is 60 dB below the peak level.

---

* A formal treatment of the Hilbert Transform is beyond the scope of this paper. Interested readers are referred to [3], [4] and [5].

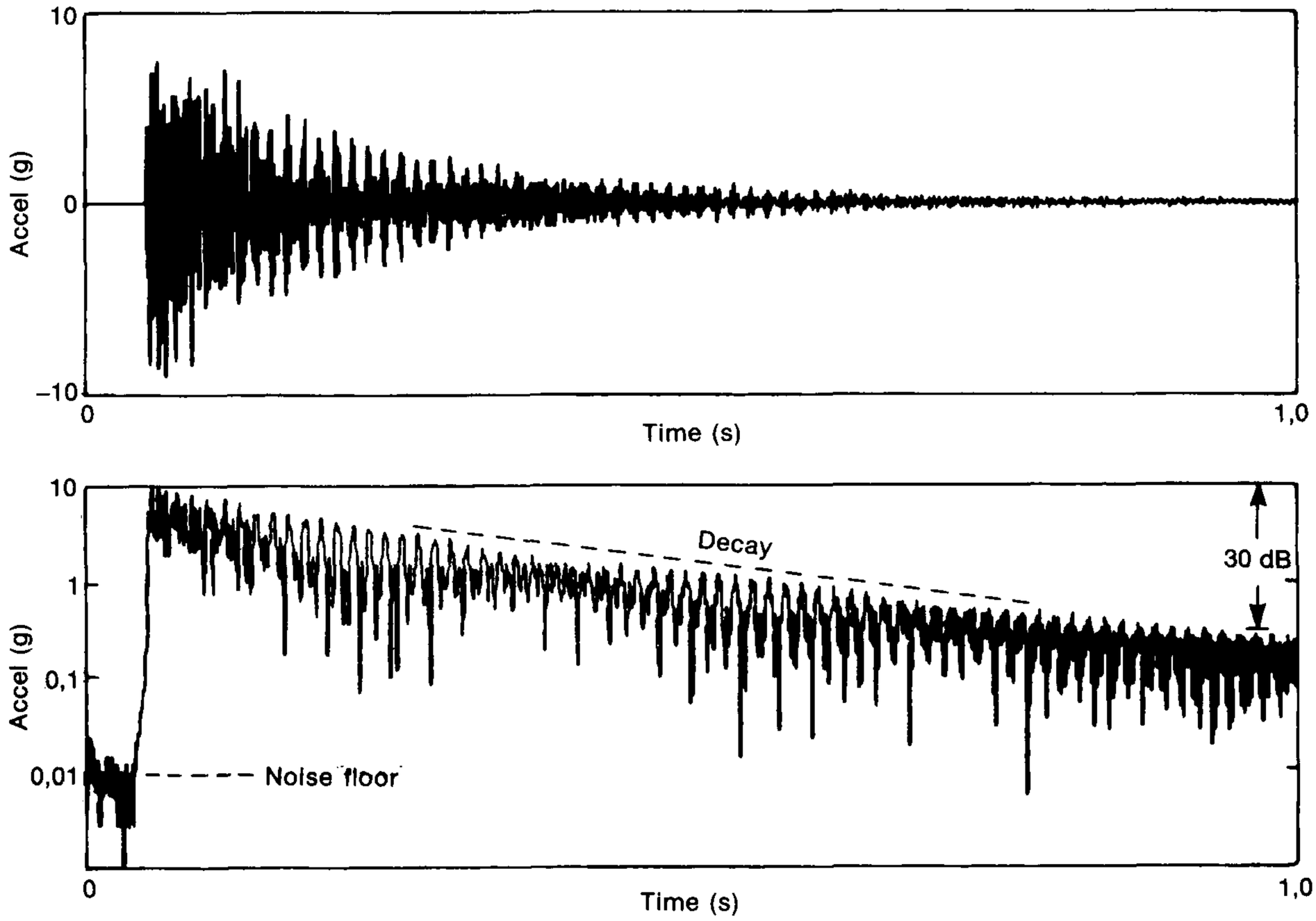

Fig. 6. a) Typical response signal
b) Magnitude function of response signal
c) Magnitude function of response signal multiplied by exponential window

Having evaluated the decay of the response signal, an optimum decay rate for an exponential window can be selected. A good rule of thumb is to weight the response so that it decays at least to the level of the noise floor of the response channel. A formula for determining the decay constant for the window is

$$\tau(\text{seconds}) = 8{,}7\,(T/L)$$

where T = analyzer time record length in seconds
L = additional change in level in decibels required at the end of the time record.

Fig.6(c) shows the response signal multiplied by a window with a decay constant of 0,3 seconds providing an additional 30 dB of decay.

Fig.7 compares frequency response functions measured with and without an exponential window. The window improves the frequency response by shaping the resonance peaks, reducing noise, and clearly defining anti-resonances. The improvements are most pronounced for low frequencies since the low frequency modes usually decay slowest.

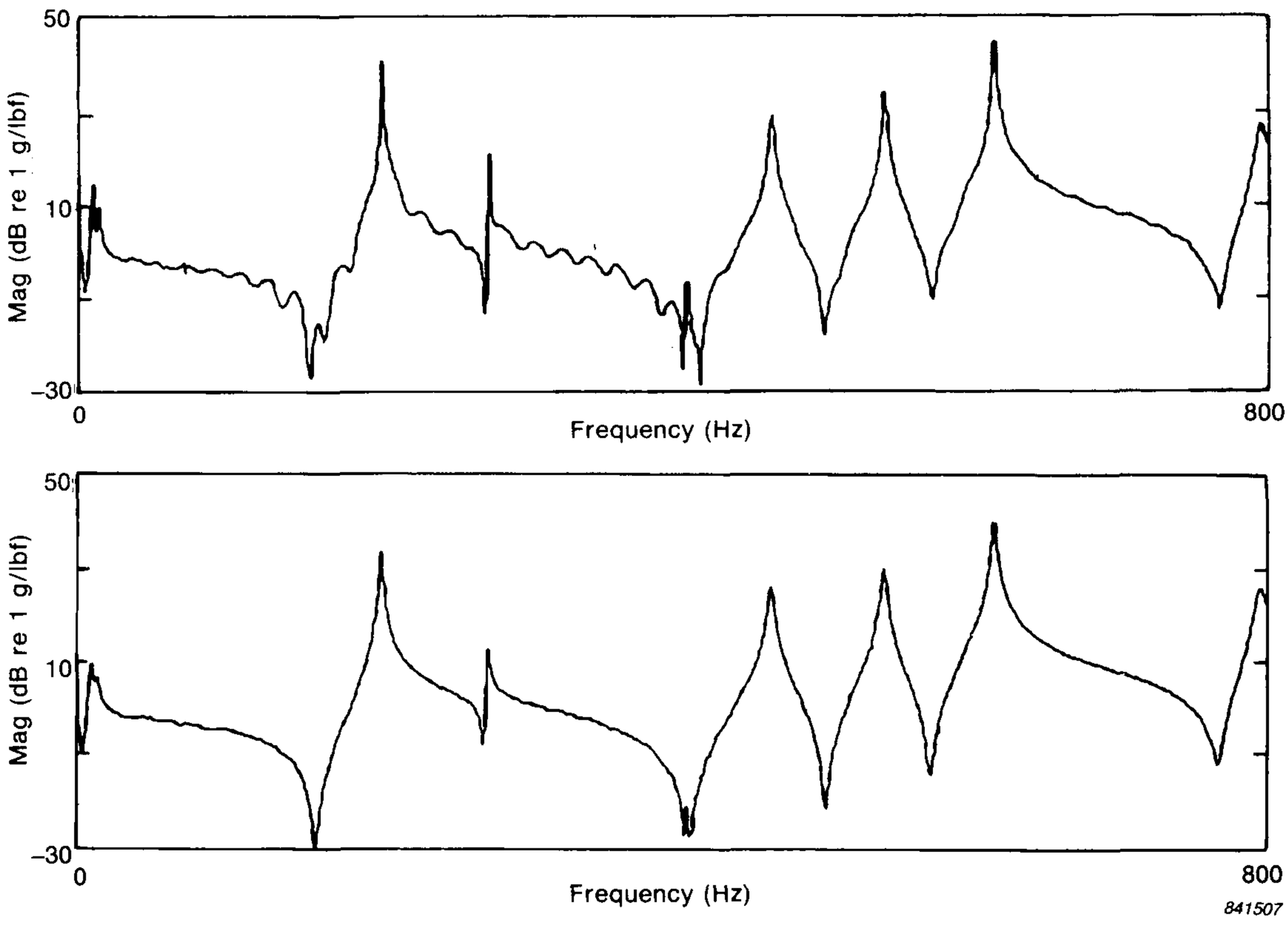

Fig. 7. Frequency response function estimated
a) without and
b) with an exponential window

Special considerations for long time records

When using an exponential window, adding extra decay has the effect of reducing the amplitude of resonance peaks and coupling closely spaced modes in the frequency response. This makes modal analysis more difficult. It is emphasized that it is better measurement procedure to use a longer time record and capture the complete response, rather than use an exponential window. Longer time records can be obtained by selecting a lower full scale frequency or using zoom analysis.

When zoom analysis is used, or for heavily damped structures, the response signal may decay well before the end of the time record. An example is shown in Fig.8. The end of the response is easily identified by the intersection of the negative sloped decay line and the horizontal noise floor. An exponential window is not needed in this case. It is more suitable to use a long force window which encompasses the complete response and eliminates the noise in the second half of the time record. When the force window is applied to the response channel a more general term for the window is "transient window".

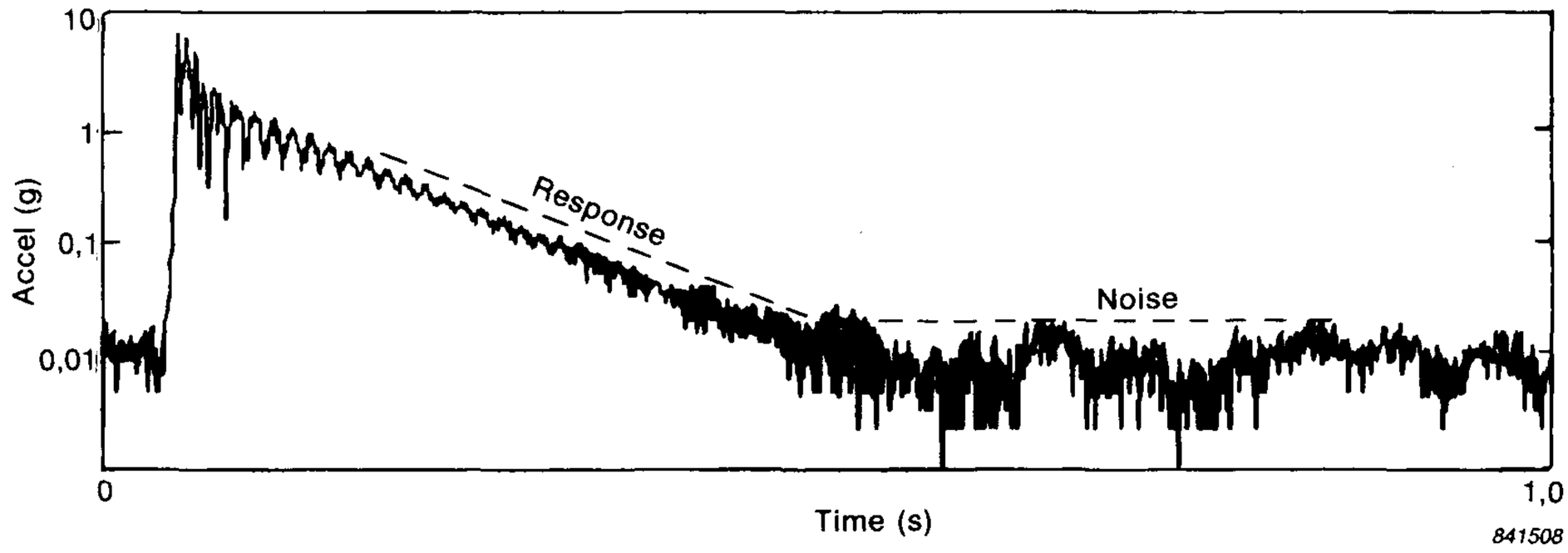

Fig. 8. Magnitude function of response signal for a heavily damped structure

When performing impact testing at very low frequencies or when using narrow zoom ranges the analyzer time record becomes excessively long. For example, an 800 line, 50 Hz analysis requires a record length of 16 seconds. Impacting a structure once every 16 seconds inputs little energy into the structure and makes modal testing a slow process.

A more efficient excitation technique is to use a series of randomly spaced impacts in each time record. Fig.9 shows example force and response signals obtained using this method. A frequency response

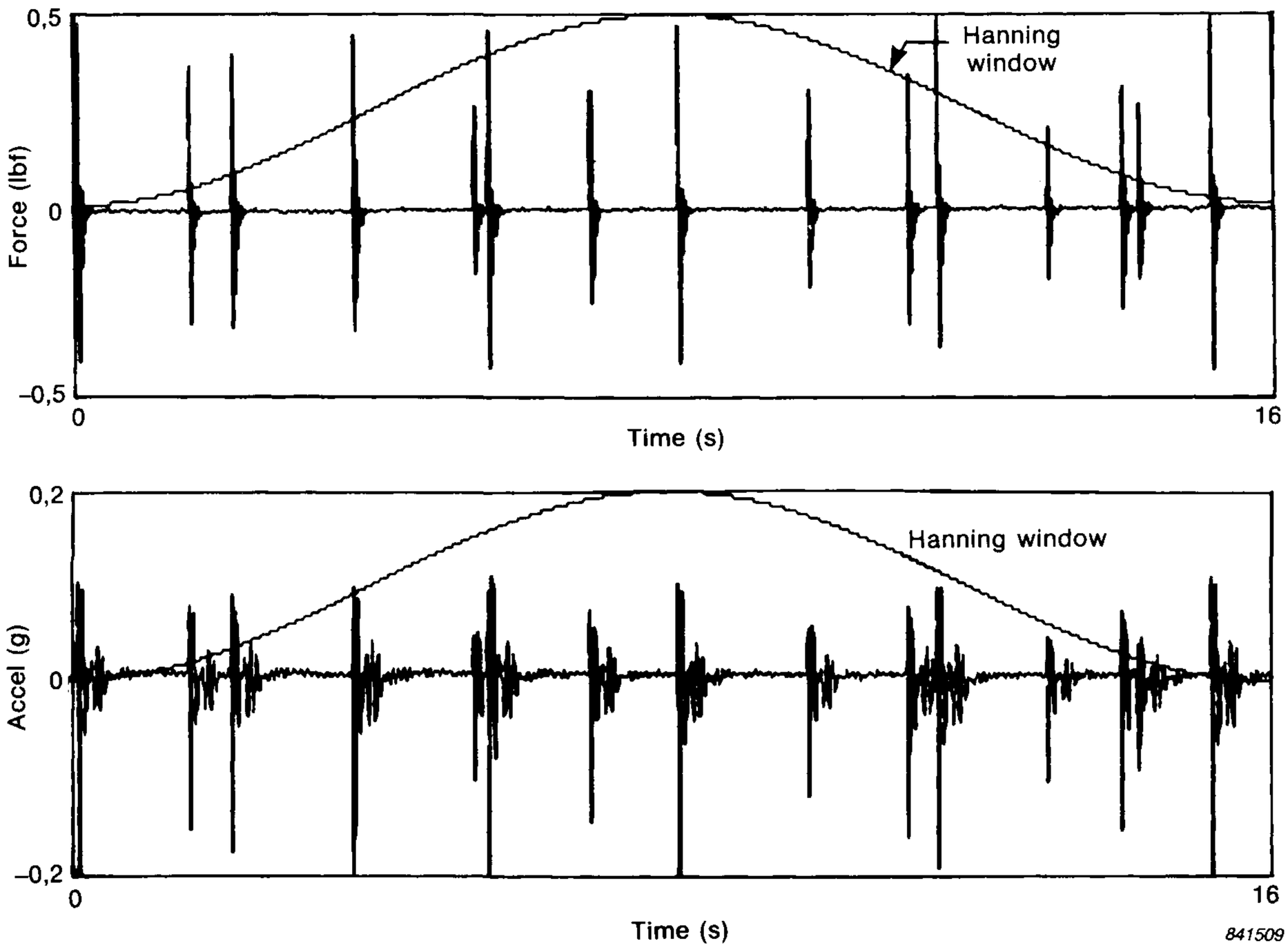

Fig. 9. Typical signals obtained using the random impact method
a) Force
b) Response

function can be estimated from an average using several such time records. This technique is referred to as random impact method. The method inputs more energy into the structure and speeds up the modal test. An additonal benefit is that it allows the use of smaller impact hammers on large structures.

The transient window designed for a single impact is not appropriate in this case, since the noise problem has been solved by adding more signal. The additional energy in decibels is equal to 10log(N) where N is the number of impacts in the record. A suitable window for both channels is the Hanning window. Use of a Hanning window avoids truncating the signal at the ends of the time record to reduce leakage in the frequency domain.

Summary

Improved measurement results are obtained by using special windows to reduce noise and leakage when performing impact tests. Careful inspection of the force and response signals should be performed before applying the windows. Filter ringing in the force channel should be included by the force window. The decay rate of the response signal should be evaluated in order to select an exponential window with an optimum decay rate.

At low full scale frequencies or when using zoom analysis, the analyzer time record length increases so that noise becomes a predominant problem. When the record length is so long that the response decays well before the end of the record a transient window should be used to reduce noise. For measurement situations with very long record lengths it may be more advantageous to circumvent the noise problem by using the random impact method. This method requires a Hanning window on both channels.

References

[1] HALVORSEN W. G. & BROWN, D. L. "Impulse Technique for Structural Frequency Response Testing", Sound and Vibration, Vol.11, No.11, 1977

[2] CORELLI, D. & BROWN, D. L. "Impact Testing Considerations", Proceedings of the 2nd International Modal Analysis Conference, Vol.2, p. 735, 1984

[3] OPPENHEIM, A. V. & SCHAFER, R. W. "Digital Signal Processing", Prentice-Hall, Inc., Englewood Cliffs, NJ, c. 1975

[4] BIERING, H. & PEDERSEN, O. Z. "System Analysis and Time Delay Spectrometry (Part 1), B&K *Technical Review*, No.1 – 1983

[5] THRANE, N. "The Hilbert Transform", B&K *Technical Review*, No.3 – 1984

COMPUTER DATA ACQUISITION FROM B&K DIGITAL FREQUENCY ANALYZERS 2131 / 2134 USING THEIR MEMORY AS A BUFFER

by

Richard J. Fridrich

ABSTRACT

When using a computer to read spectra from a Digital Frequency Analyzer 2131 or a Sound Intensity Analyzer 2134, not all of the data can be transferred, if the computer is not fast enough. To overcome this problem, the analyzer's memory can be used as a buffer for the computer, to transfer data to the computer's memory and thence to its disk storage. The algorithm presented in this article shows how this is achieved on a MINC–11 computer.

SOMMAIRE

Lorsque l'on fait lire par un ordinateur le spectre contenu dans un Analyseur de fréquence numérique 2131 ou un Analyseur d'intensité acoustique 2134, il se peut, si l'ordinateur n'est pas suffisamment rapide, que toutes les données ne puissent être transférées. Pour éviter ce problème, la mémoire de l'analyseur peut être utilisée comme mémoire tampon pour l'ordinateur, afin de transférer les données vers l'ordinateur puis vers le disque de stockage. L'algorithme présenté dans cet article montre comment cela est réalisé sur un ordinateur MINC–11.

ZUSAMMENFASSUNG

Bei der Überführung von Spektren vom digitalen Terz/Oktav-Analysator 2131 oder dem Schallintensitätsanalysator 2134 an einen Rechner, gehen Daten verloren, wenn der Rechner zu langsam ist. Um dieses Problem zu lösen, läßt sich der Speicher des Analysators als Puffer für den Rechner einsetzen, um die Daten an den Speicher des Rechners und weiter an einen Plattenspeicher zu überführen. Der in diesem Artikel beschriebene Algorithmus zeigt das Verfahren am Beispiel eines MINC-11-Rechners.

Introduction

Not all computers having an IEC or IEEE bus have the ability to read spectra from the B&K 2131 Digital Frequency Analyzer or 2134 Sound Intensity Analyzer as fast as Hewlett-Packard 200 series Desk-Top Calculators. This handicap often means important data are lost during the time that the computer is reading a spectrum. The algorithm presented here can overcome this handicap, at least for measurements using linear averaging, by using the analyzer's memory as a buffer for the computer.

Data transfer from the analyzer to the computer's memory can then take place while the next linear average is being acquired. In addition, before the next linear average is completed a second data transfer can be made from the computer's memory to its disk storage. An important advantage results from this second transfer, because the maximum number of spectra that can be acquired is now limited only by the capacity of disk storage rather than the memory of the computer.

Because a large number of linearly averaged spectra can be stored on a disk, this algorithm can be useful in community noise studies where spectral analysis as well as linear averaging are desired for extended periods of time. In addition, this algorithm can be used to extend the effective averaging times beyond the binary sequence available on the 2131 or 2134 for applications using linear averaging greater than one second long.

Detailed Algorithm Description

While this algorithm is general in nature, it is presented here as implemented in the programming language BASIC for a Digital Equipment Corporation MINC-11. The partial program listing, given at the end of this brief article, contains only the algorithm for controlling the 2131 and omits the details for dimensioning arrays or opening and closing disk files which are required for a complete program. Remark statements for program documentation are included on most of the lines following a backslash (\) which is used in MINC-11 BASIC to separate multiple statements on the same program line. For clarity of presentation, each line contains only one executing statement.

Initialization

The listing begins on lines 870 and 880 with the specification of the bus talk and listen addresses for the 2131 or 2134. The next two lines require

the user to enter at the computer keyboard the time interval over which data will be acquired. Because this program commands the analyzer to perform a series of one second linear averages, the value that the user enters is also the number of spectra that will be acquired. The command to set the averaging control to one second (remote programming code "08", see Table 4.2 in the Instruction Manual for the 2131 or 2134) is sent to the analyzer in line 910 which is the beginning of the initial analyzer setup sequence. If this command is changed so that a different averaging time is selected, the data acquisition time will correspond to the product of the selected averaging time and number of spectra to be acquired given in variable 19.

The initial analyzer setup sequence (lines 910 to 940) places the 2131 or 2134 in the proper mode for data acquisition, by not only setting the averaging time and mode, but also initializing the analyzer's memory and displaying the stored spectrum, so that when the data acquisition starts the computer can read the stored spectrum while new data are accumulating in the input spectrum memory. This is the key to the algorithm which allows input to the analyzer while simultaneously reading the stored spectrum.

Lines 950 to 990 are the final commands before data acquisition begins. At this point the variable for counting the number of acquired spectra is initialized and the user is alerted that data acquisition is initiated by typing a carriage return. The final step in the initialization sequence is to reset the averaging control so that the averager is clear of old data.

Data Acquisition

Data acquisition begins at line 1000 with the command for the averaging control to proceed ("M = "). As the analyzer begins a one second linear average, the program enters a two line loop which reads the status of the averager at line 1010 and tests for the stop condition (">") in line 1020. This short loop takes up the slack in the timing between the analyzer and the computer. While the computer is in this loop, the analyzer is acquiring data, but its display will not show the linear averaging process because the stored spectrum was selected for display earlier. When the stop condition is sensed, the computer commands the analyzer to store the resultant spectrum ("H > ") causing it to appear on the analyzer's display. In the next two lines, 1040 and 1050, the averaging control is reset ("M ? ") to clear it of the old data and then is commanded to proceed ("M = ") so that the data acquisition can continue. At this point the analyzer is both acquiring the next one second

linear average, and displaying the previously acquired average in preparation for transfer to the computer.

Data Transfer

Lines 1060 to 1110 perform the data transfer first from the analyzer to the computer's memory and then from the computer's memory to disk. To initiate the transfer the analyzer's output control is set to digital ("E ? ") at line 1060. Then in lines 1070 and 1080 the computer receives the displayed spectrum from the analyzer. This transfer takes two lines because MINC-11 BASIC sets the maximum length for a string variable at 256 characters. This limit necessitates receiving the output spectrum in two fragments. Because this program was written to control a 2131 with the WH0490 two channel extension, each output spectrum consists of 45 channels of 7 characters each (2131 or 2134 data format 1) for a total of 315 characters. The length of the two fragments received by the MINC-11 were arbitrarily set at 84 and 231 (the lengths specified in the RECEIVE statements are 83 and 230 respectively, because the first value of an index for the MINC-11 is labeled zero). After the output spectrum has been received by the computer, the analyzer's output control is set to stop ("E = ") in line 1090. Finally, the output spectrum is transferred from the computer's memory to disk in lines 1100 and 1110, where the two fragments of the received data are written to two separate arrays on disk.

Algorithm Completion

The final steps of the algorithm are completed in lines 1120 to 1160 where the counter is incremented and tested to see if the desired number of spectra have been acquired. The PRINT statement in line 1130 of this program is a non-essential but useful statement since it gives the user feedback on the progress of the program. It can be omitted for faster execution. Since the entire purpose of this algorithm is to obtain more than one spectrum, the data acquisition and transfer process will normally be repeated several times before the test condition of the IF statement at line 1140 becomes true. To repeat the process the computer will need to return to checking the status of the averaging control for the stop condition. However, since the analyzer's output control was the last function controlled by the computer, the averaging control's function code "M" must be sent in line 1150 without any setting code, so that the proper function is being sensed when the computer is sent to line 1010 by the GO TO statement at line 1160.

Data Losses

When the computer again starts checking the averaging control status at line 1010, the analyzer should not have completed taking the next one second average, so that no data are lost during the transfer process. The only place that data will be lost is during the execution of lines 1010 through 1050 between the time when the stop condition is first received, and the averaging control is commanded to proceed after storing the spectrum and resetting the averager. For the MINC-11 this time interval is about 0,06 seconds. During proper program operation the sensing lights for the stop and reset buttons of the averaging control should briefly flicker as these program lines are executed. This data acquisition process can continue for as long as desired or until the storage capacity of the disk is exhausted.

Partial Program Listing

```
870 A1% = 16                    \ REM ** BUS TALK ADDRESS FOR B&K 2131
880 A2% = 17                    \ REM ** BUS LISTEN ADDRESS FOR B&K 2131
890 PRINT 'ENTER ACQUISITION TIME IN SECONDS';
900 INPUT 19                    \ REM ** 19 IS  #  OF SPECTRA TO BE ACQUIRED
910 SEND('08',A2%)              \ REM ** SET AVERAGING TIME TO 1 SECOND
920 SEND('L?',A2%)              \ REM ** SET AVERAGING START TO LINEAR
930 SEND('H>',A2%)              \ REM ** SET MEMORY FUNCTION TO STORE
940 SEND('G<',A2%)              \ REM ** SET OUTPUT CONTROL TO STORED SPECTRUM
950 I = 0                       \ REM ** ZERO THE COUNTER
960 PRINT 'ANALYZER SET FOR LINEAR AVERAGING, STORED SPECTRUM DISPLAYED'
970 PRINT 'TYPE RETURN WHEN READY TO BEGIN';
980 LINPUT Q$                   \ REM ** COMPUTER WAITS FOR ENTRY FROM KEYBOARD
990 SEND(M?,A2%)                \ REM ** SET AVERAGING CONTROL TO RESET
1000 SEND('M = ',A2%            \ REM ** SET AVERAGING CONTROL TO PROCEED
1010 RECEIVE(A$,,17)            \ REM ** READ THE AVERAGING CONTROL CODE
1020 IF AS<>'>' THEN 1010       \ REM ** CHECK AVERAGING CONTROL FOR STOP CONDITION
1030 SEND('H>',A2%)             \ REM ** WHEN STOPPED, STORE SPECTRUM IN MEMORY
1040 SEND('M?',A2%)             \ REM ** SET THE AVERAGING CONTROL TO RESET
1050 SEND('M=',A2%)             \ REM ** SET THE AVERAGING CONTROL TO PROCEED
1060 SEND('E?',A2%)             \ REM ** SET OUTPUT CONTROL TO DIGITAL
1070 RECEIVE(S1$,83,A1%)        \ REM ** READ THE FIRST PART OF THE SPECTRUM
1080 RECEIVE(S2$,230,A1%)       \ REM ** READ THE SECOND PART OF THE SPECTRUM
1090 SEND('E=',A2%)             \ REM ** SET THE OUTPUT CONTROL TO STOP
1100 R1$(I)=S1$                 \ REM ** TRANSFER THE SPECTRUM FIRST PART TO DISK
1110 R2$(I)=S2$                 \ REM ** TRANSFER THE SPECTRUM SECOND PART TO DISK
1120 I=I+1                      \ REM ** INCREMENT THE COUNTER
1130 PRINT I                    \ REM ** DISPLAY THE COUNTER
1140 IF I>=19 THEN 3000         \ REM ** IF ENOUGH SPECTRA HAVE BEEN ACQUIRED, STOP
1150 SEND,('M',A2%)             \ REM ** PREPARE TO SENSE AVERAGING CONTROL STATUS
1160 GO TO 1010                 \ REM ** IF MORE SPECTRA NEEDED, START AGAIN
3000 PRINT 'DATA ACQUISITION COMPLETED'
```

Impact Hammer Type 8202

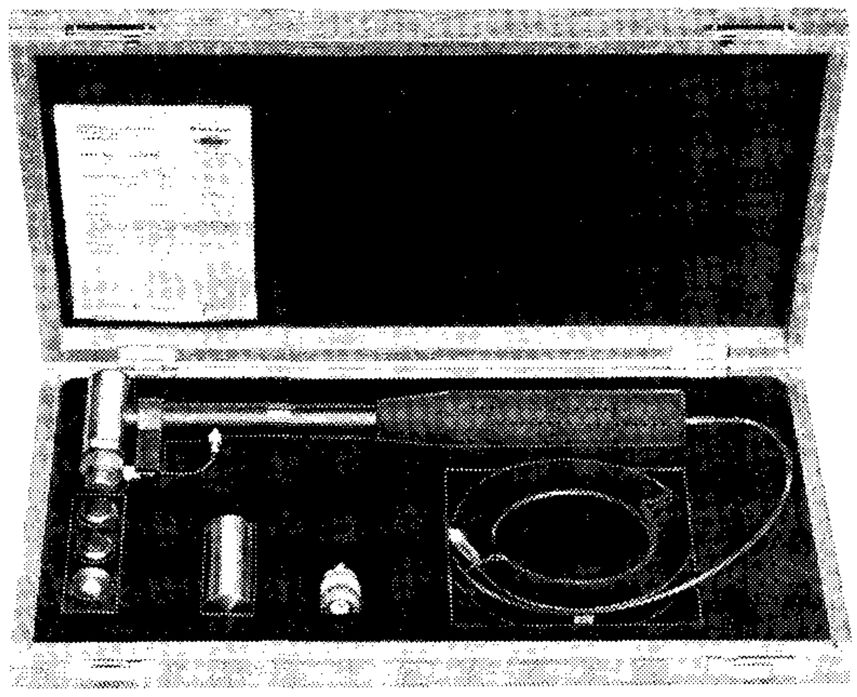

The Impact Hammer, Type 8202, is an instrumented hammer for testing structural behaviour in conjunction with a dual- or multi-channel spectrum analyzer. The force applied to the structure is measured by the built-in, individually calibrated Force Transducer Type 8200, while the structural response is measured with a separate accelerometer fitted to the test object. The three different tips (steel, plastic and rubber) supplied with the 8202 enable the pulse duration to be varied from 0,2 ms to 5 ms with a maximum force of 5000 N on a massive, hard object. Typical applications of the Impact Hammer with a B&K Dual Channel Analyzer Type 2032 or 2034 are impact testing (for determining frequency response functions) and as part of a dynamic structural testing system (for mechanical mobility and impedance measurements, for modal analysis and for the simulation of structural response).

Force Transducer Type 8201

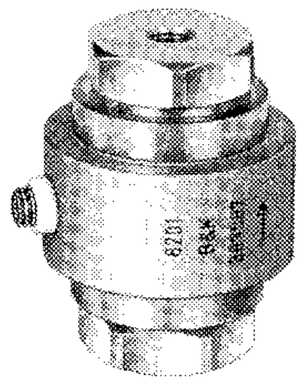

The Force Transducer Type 8201 is a larger version of the Type 8200 with the added features of a larger force range and low sensitivity to bending moment and transverse forces. It is designed to measure dynamic, short duration static and impact, tensile and compressive forces in machinery and other constructions. When used together with an accelerometer and vibration exciter it is well suited for controlling the applied force in measurements of mechanical impedance.

The principal feature of this transducer is that the upper and lower preloading nuts can be removed enabling the transducer to be used as a load washer in compressive force measurements. After remounting the preloading nuts, the calibration is, however, still valid. Tensile forces of 4000 N (900 lbf) and compressive forces of 16000 N (3600 lbf) can be measured when the preloading nuts are mounted, while as a load washer alone compressive forces up to 20,000 N (4500 lbf) are measurable.

The transducer can be used under severe environmental conditions on account of its rugged, all welded, hermetically sealed construction and because of its ceramic insulated micro-plug connector sealed with moulded glass. The allowable temperature range is –196°C to 150°C.

Calibration Exciter Type 4294

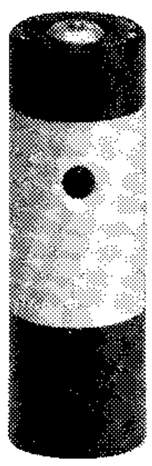

For rapid calibration and checking of vibration measurement, monitoring and recording systems, Brüel & Kjær has developed a hand-held battery-powered vibration reference source, the Calibration Exciter Type 4294.

It is intended for use with piezoelectric accelerometers and other types of vibration transducers having a mass up to 70 grammes. It permits accurate calibration and adjustment of measuring instrumentation at a reference vibration level of $10\,ms^{-2}$ at a frequency of 159,2 Hz ($1000\,rad\,s^{-1}$). Calibration may additionally be carried out at constant velocity and displacement levels of $10\,mms^{-1}$ and $10\,\mu m$ respectively.

The 4294 operates as an electromagnetic exciter driven by a stabilized oscillator. A highly accurate, constant vibration level is maintained using a built-in accelerometer to provide servo feedback. Overload is prevented by automatic power cut-off if the accelerometer mass exceeds the maximum 70 grammes.

Rhino-Larynx Stroboscope Type 4914

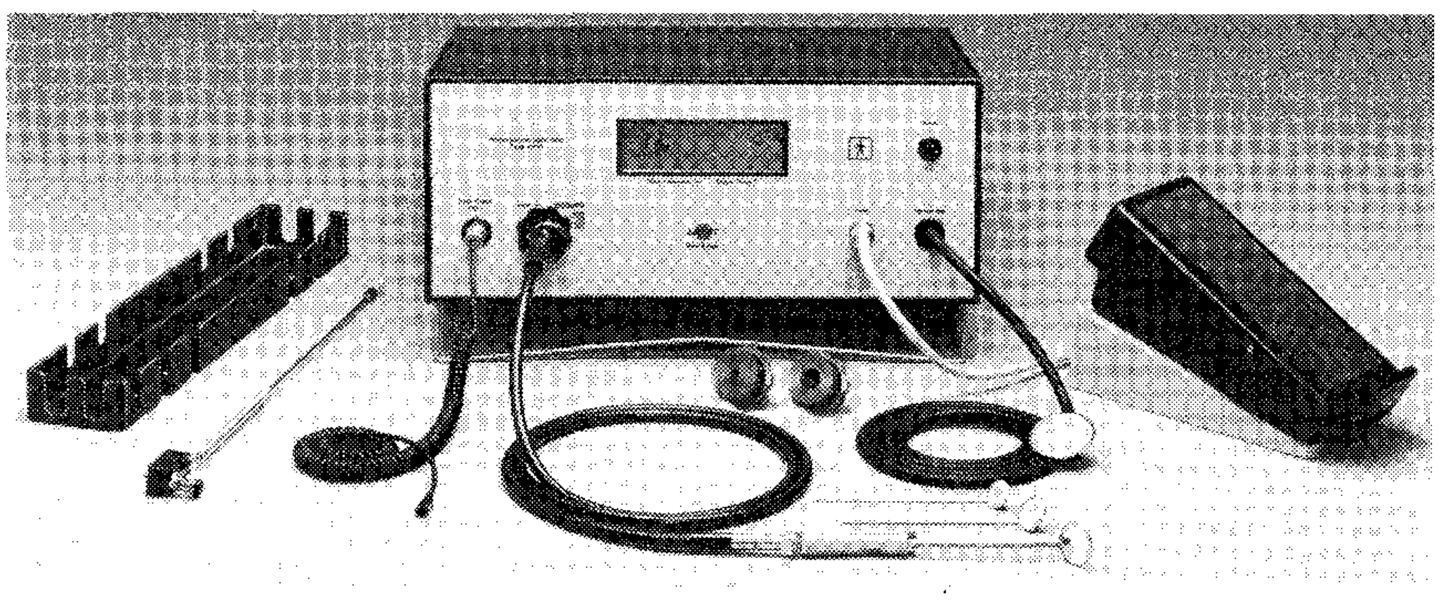

The Rhino-Larynx Stroboscope Type 4914 provides doctors, speech therapists, music teachers and other specialists in ENT fields with a user-friendly instrument for comprehensive visual examination of the larynx, upper respiratory tract and sinuses. The 4914 combines a stroboscope, fixed light source and frequency counter in a single unit and embodies more than 15 years' experience in the design of instrumentation for clinical applications. The unit is easily operated, with pedal control of all functions and a large self-explanatory display, enabling the specialist to quickly master the instrument and concentrate on the physiological factors of interest.

The powerful stroboscopic and fixed light sources of the 4914 provide excellent illumination for direct observation, as well as colour video recording through flexible fibrescopes. Connection to an operation microscope is also possible. Hygiene requirements are easily met and the 4914 complies with Safety Class II of IEC 601–1 (Type BF).

Photoelectric Tachometer Probe Type MM 0024

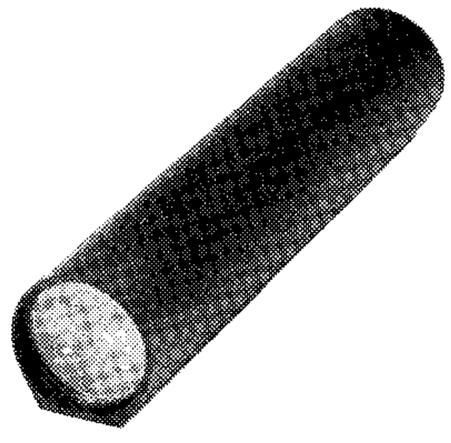

The Tachometer Probe, MM 0024 is a small, handy device designed to facilitate the remote triggering of vibration analysis and balancing equipment in synchronism with rotating and reciprocating machine parts. A special benefit is that it can operate up to 800 mm from the target, and thus at a safe distance from moving parts or otherwise hazardous environments.

The MM 0024 generates a modulated infra-red beam and has a small indicator to confirm correct orientation with the target. Light reflected back from a piece of self-adhesive reflective tape attached to the rotating or reciprocating part produces a well-defined pulse-train corresponding precisely to the cyclic movement of the object. This provides a stable constant-magnitude trigger signal directly suited for triggering B&K equipment such as the Portable Balancing Sets Types 3517 and 9537, Tracking Filter Type 1623 and Stroboscope Type 4912.

The probe is equipped with a combined signal/power cable for coupling the probe to these battery-powered instruments, and a thread for attaching it to a tripod or magnetic foot.

PREVIOUSLY ISSUED NUMBERS OF BRÜEL & KJÆR TECHNICAL REVIEW

(Continued from cover page 2)

1-1978 Digital Filters and FFT Technique in Real-time Analysis.
4-1977 General Accuracy of Sound Level Meter Measurements.
Low Impedance Microphone Calibrator and its Advantages.
3-1977 Condenser Microphones used as Sound Sources.
2-1977 Automated Measurements of Reverberation Time using the Digital Frequency Analyzer Type 2131.
Measurement of Elastic Modulus and Loss Factor of PVC at High Frequencies.
1-1977 Digital Filters in Acoustic Analysis Systems.
An Objective Comparison of Analog and Digital Methods of Real Time Frequency Analysis.
4-1976 An Easy and Accurate Method of Sound Power Measurements.
Measurement of Sound Absorption of rooms using a Reference Sound Source.
3-1976 Registration of Voice Quality.
Acoustic Response Measurements and Standards for Motion-Picture Theatres.
2-1976 Free-Field Response of Sound Level Meters.
High Frequency Testing of Gramophone Cartridges using an Accelerometer.
1-1976 Do We Measure Damaging Noise Correctly?

SPECIAL TECHNICAL LITERATURE

As shown on the back cover page, Brüel & Kjær publish a variety of technical literature which can be obtained from your local B & K representative.
The following literature is presently available:

Mechanical Vibration and Shock Measurements (English), 2nd edition
Acoustic Noise Measurements (English), 3rd edition
Architectural Acoustics (English)
Strain Measurements (English, German)
Frequency Analysis (English)
Electroacoustic Measurements (English, German, French, Spanish)
Catalogs (several languages)
Product Data Sheets (English, German, French, Russian)

Furthermore, back copies of the Technical Review can be supplied as shown in the list above. Older issues may be obtained provided they are still in stock.

Printed in Denmark by Nærum Offset

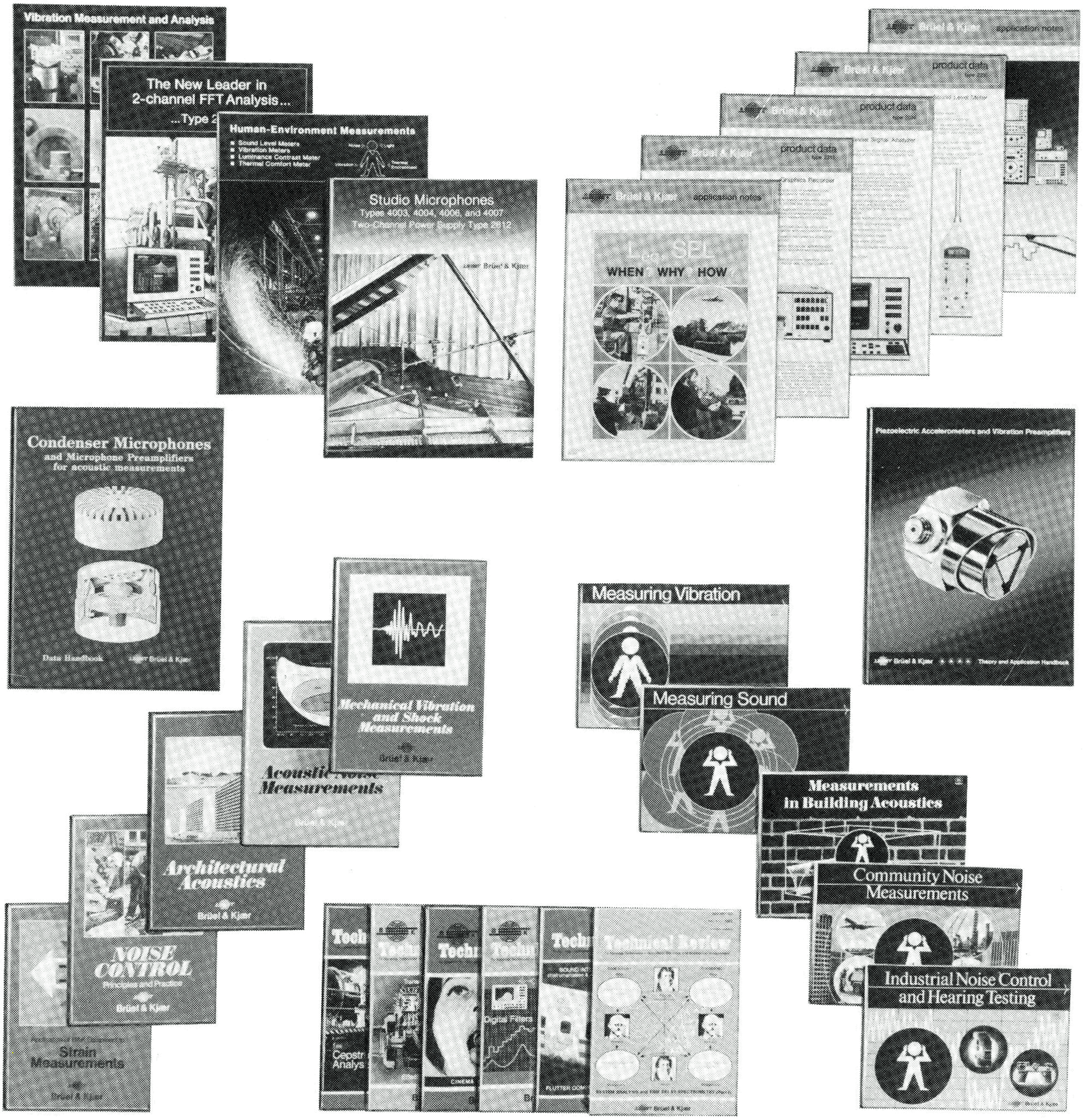

BV 0016-11

Brüel & Kjær

DK-2850 NÆRUM, DENMARK · Telephone: + 45 2 80 05 00 · Telex: 37316 bruka dk